2180 J. Am. Chem. Soc. 1986, 108, 2180-2191

Bonding in Transition-Metal-Methylene Complexes. 2. $(RuCH_2)^+$, a Complex Exhibiting Low-Lying Methylidene-like and Carbene-like States[1]

Emily A. Carter† **and William A. Goddard III***

Contribution No. 7266 from the Arthur Amos Noyes Laboratory of Chemical Physics, California Institute of Technology, Pasadena, California 91125. *Received August 15, 1985*

Abstract: The electronic structure for a representative late-transition-metal-methylene complex, $Ru{=}CH_2^+$, has been studied by ab initio methods (generalized valence bond/configuration interaction). The electronic-state spectrum reveals five states close in energy (spread of 12.9 kcal/mol) that partition into two groups in terms of energy separation and mode of metal-carbon bonding. The ground state has $^2A_2$ symmetry and contains covalent M–C σ and π bonds ("metal-methylidene"); a $^2A_1$ state of the same bond character is only 1.2 kcal/mol higher. A cluster of three degenerate excited states ($^4A_2$, $^4B_1$, and $^4B_2$) 12.9 kcal/mol above the ground state exhibits completely different bonding character, namely, σ-donor/π-acceptor M–C bonds are formed ("metal-carbene"). We conclude that for highly unsaturated, late-transition-metal systems, metal-carbene bonding may be competitive with metal-alkylidene bonding, leading to donor/acceptor bonds comparable in strength to that of covalent double bonds!

I. Introduction

Metal complexes containing CH_2 ligands have been postulated as intermediates for numerous catalytic reactions (e.g., Fischer–Tropsch reductive polymerization of CO and olefin metathesis) and have been isolated in a number of cases including[2a,b]

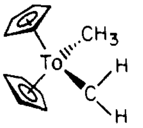

1

ond

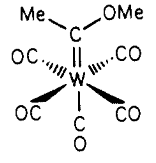

2

In the simple oxidation-state formalism, the CH_2 is thought of as $(CH_2)^{2-}$, with the metal oxidized by two units; however, the chemistry of these systems tends to fall into one of two distinct classes, one of which is nucleophilic and the other electrophilic.

A series of generalized valence bond (GVB) studies on high-oxidation-state metal complexes such as[3] $Cl_2Ti{=}CH_2$ (**3**), $Cl_4Cr{=}CH_2$ (**4**), and $Cl_4Mo{=}CH_2$ (**5**) showed that these systems all have the form **6** with a *covalent metal-carbon double bond*

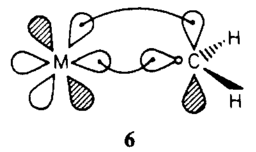

6

involving a π bond composed of one electron in a metal dπ orbital spin-paired with one electron in a C pπ orbital, and a σ bond consisting of one electron in a metal dσ orbital spin-paired with one electron in a C sp^2 σ orbital. Similar studies[1,4] on $(Cr{=}CH_2)^+$ (**7**), $(Mn{=}CH_2)^+$ (**8**), and $(Fe{=}CH_2)^+$ (**9**) lead also to a double bond with a similar covalent M dπ–C pπ bond but a σ bond having varying amounts of dσ and sσ character on the metal.

Such studies suggest the following valence bond view of metal-methylene bonds. The metal is considered to be in the atomic configuration (s^1d^{n-1}, d^n, etc.) appropriate for its charge and environment (no formal charge transfer to the CH_2), and the CH_2 is considered to be neutral and in one of its two most stable forms, the triplet $\sigma\pi$ ground state **10** or the singlet σ^2 excited state (9 kcal/mol higher[5]) **11**. The ground state and low-lying excited states of the system are formed by combining the various low-lying metal atomic configurations with **10** and **11** to form various bonding states.

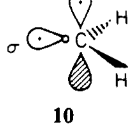

10

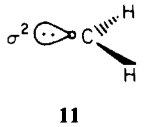

11

Metal-methylene complexes involving **10** have covalent metal-carbon double bonds and are termed metal methylidenes to emphasize the double-bond character. Examples include the so-called Schrock complexes **1**. Metal-methylene complexes involving **11** require empty dσ or s orbitals on the metal (that can accommodate the CH_2 σ pair) and prefer a doubly occupied dπ orbital on the metal that can overlap the empty π orbital of σ^2 CH_2. This leads to a metal-carbon bond best described in terms of donor-acceptor or Lewis acid-Lewis base concepts (as in "Fischer"-type carbenes such as **2**, or, in general, as **12**). We

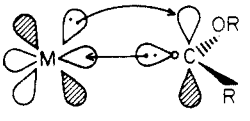

12

will refer to such systems as metal carbenes. Supporting evidence for such differences in the metal-carbon bond character is the drastic contrast in chemical reactivity of **6** with **12**. Metal methylidenes such as **3–5** are precatalysts for metathesis[6] and polymerization reactions with olefins,[7] whereas metal carbenes such as **2** generally exhibit stoichiometric reactivity with olefins, leading to the formation of cyclopropanes.[8]

---

† National Science Foundation Predoctoral Fellow, 1982–1985.

(1) Paper 1 in this series: Carter, E. A.; Goodard, W. A., III. *J. Phys. Chem.* **1984**, *88*, 1485.

(2) (a) Schrock, R. R. *J. Am. Chem. Soc.* **1975**, *97*, 6577. Guggenberger, L. J.; Schrock, R. R. *Ibid.* **1975**, *97*, 6578. (b) Fischer, E. O. *Adv. Organomet. Chem.* **1976**, *14*, 1. For an extensive review of both Fischer- and Schrock-type carbenes, Dötz, K. H.; Fischer, H.; Hofmann, P.; Kreissl, F. R.; Schubert, U.; Weiss, K. *Transition Metal Carbene Complexes*; Verlag Chemie: Deerfield Beach, FL, 1984.

(3) (a) Rappé, A. K.; Goddard, W. A., III. In *Potential Energy Surfaces and Dynamics Calculations*; Truhlar, D. G., Ed.; Plenum: New York, 1981; pp 661–684. (b) *J. Am. Chem. Soc.* **1982**, *104*, 297. (c) *Ibid.* **1982**, *104*, 448. (d) *Ibid.* **1980**, *102*, 5114.

(4) $MnCH_2^+$ and $FeCH_2^+$ work: Brusich, M. J.; Goddard, W. A., III, to be published. For another recent paper on $CrCH_2^+$ concurring with our earlier results (ref 1), see Alvarado-Swaisgood, A. E.; Allison, J.; Harrison, J. F. *J. Phys. Chem.* **1985**, *89*, 2517.

(5) Leopold, D. G.; Murray, K. K.; Lineberger, W. C. *J. Chem. Phys.* **1984**, *81*, 1048.

(6) (a) Lee, I. B.; Ott, K. C.; Grubbs, R. H. *J. Am. Chem. Soc.* **1982**, *104*, 7491. (b) Wengrovius, I. A.; Schrock, R. R.; Churchill, M. R.; Missert, I. R.; Youngs, W. I. *Ibid.* **1980**, *102*, 4515. (c) Gilet, M.; Mortreux, A.; Folest, J.-C.; Petit, F. *Ibid.* **1983**, *105*, 3876. (d) Kress, J.; Osborn, J. A. *Ibid.* **1983**, *105*, 6346. (e) Katz, T. J.; Han, C.-C. *Organometallics* **1982**, *1*, 1093. (f) Howard, T. R.; Lee, J. B.; Grubbs, R. H. *J. Am. Chem. Soc.* **1980**, *102*, 6876.

(7) (a) Turner, H. W.; Schrock, R. R. *J. Am. Chem. Soc.* **1982**, *104*, 2331. (b) Levisalles, J.; Rose-Munch, F.; Rudler, H.; Daran, J.-C.; Dromzée, Y.; Jeannin, Y. *J. Chem. Soc., Chem. Commun.* **1981**, 152.

0002-7863/86/1508-2180$01.50/0

This gestalt view of bonding in terms of combining complete many-electron states is a characteristic distinguishing the valence bond viewpoint from the molecular orbital viewpoint in which one-electron orbitals are constructed (from the same atomic orbitals), but where distinctions between atomic configurations such as σ^2 vs. $\sigma\pi$ methylene or s^1d^4 vs. d^5 Cr^+ become blurred. Although this valence bond view of bonding has been implicit in several papers, no examples of the metal–carbene bonding (as in **12**) have been examined with GVB techniques. In this paper we report all-electron ab initio GVB calculations on a system $(RuCH_2)^+$ (**13**) that exhibits both methylidene- and carbene-like states having comparable bond strengths. Indeed, the lowest carbene-like state

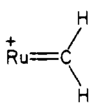

13

($^4A_2$) is only 12.9 kcal/mol above the lowest methylidene-like state ($^2A_2$). The results for the $^2A_2$ ground state of **13** (methylidene) are examined in section II, while the wave function for the $^4A_2$ excited state of **13** (carbene) is described in section III. A summary of our conclusions is presented in section IV, while further details of the calculations are outlined in section V.

II. The Ground State of $RuCH_2^+$: Methylidene Bonding

A. Low-Lying Covalent States. Using the coordinate system

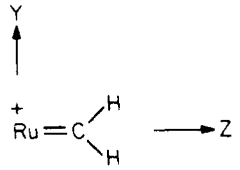

we will denote the five valence d orbitals of Ru as

$$\mathrm{d}\sigma = \mathrm{d}_{z^2} \quad (a_1)$$
$$\mathrm{d}\pi_x = \mathrm{d}_{xz} \quad (b_1)$$
$$\mathrm{d}\bar{\pi}_y = \mathrm{d}_{yz} \quad (b_2)$$
$$\mathrm{d}\delta_{xy} = \mathrm{d}_{xy} \quad (a_2)$$
$$\mathrm{d}\bar{\delta}_{x^2-y^2} = \mathrm{d}_{x^2-y^2} \quad (a_1)$$

In C_{2v} symmetry, $\mathrm{d}\bar{\delta}$ and $\mathrm{d}\sigma$ have the same symmetry (shown in parentheses); however, the $\mathrm{d}\sigma$ and $\mathrm{d}\bar{\delta}$ character perseveres. To predict low-lying states of the metal–methylene complex, we utilize the valence bond picture in which the ground-state molecular or atomic fragments are brought together to form two-electron bond pairs in the resulting complex. Starting with the high-spin d^7 configuration associated with the ^4F ground state of Ru^+ and the ground state of CH_2 (**10**), we see that singly occupied $\mathrm{d}\sigma$ and $\mathrm{d}\pi$ orbitals are required on Ru^+. This leaves three orbitals ($\mathrm{d}\delta$, $\mathrm{d}\bar{\delta}$, and $\mathrm{d}\bar{\pi}$) for the remaining five valence electrons on Ru^+. Thus, double-bonded $RuCH_2^+$ leads to three low-lying states with the following occupations of the nonbonding Ru d orbitals.

$$\begin{aligned} &^2B_2\ (\mathrm{d}\delta)^2(\mathrm{d}\bar{\delta})^2(\mathrm{d}\bar{\pi})^1\ (20.0\text{ kcal/mol above }^2A_2) \\ &^2A_1\ (\mathrm{d}\delta)^2(\mathrm{d}\bar{\delta})^2(\mathrm{d}\bar{\pi})^2\ (1.2\text{ kcal/mol above }^2A_2) \qquad (1) \\ &^2A_2\ (\mathrm{d}\delta)^1(\mathrm{d}\bar{\delta})^2(\mathrm{d}\bar{\pi})^2\ (\text{ground state}) \end{aligned}$$

Using simple ligand-field considerations, one might argue that the $^2B_2$ state would be the lowest, since the $\mathrm{d}\bar{\pi}$ orbital, which overlaps the CH bonds, is singly occupied (less electron–electron repulsion in the molecular plane than for the other two states). However, this state is 20.0 kcal/mol above the ground state. In order to consistently predict such ordering of states in the bound complex, it is useful to examine the energies for the corresponding atomic configurations of Ru^+. As shown in Table I, the three configurations in (1) lead to the following atomic energies:

$$\begin{aligned} &^2B_2\ (\mathrm{d}\sigma)^1(\mathrm{d}\pi)^1(\mathrm{d}\delta)^2(\mathrm{d}\bar{\delta})^2(\mathrm{d}\bar{\pi})^1\ (20.1\text{ kcal/mol above }^2A_2) \\ &^2A_1\ (\mathrm{d}\sigma)^1(\mathrm{d}\pi)^1(\mathrm{d}\delta)^2(\mathrm{d}\bar{\delta})^1(\mathrm{d}\bar{\pi})^2\ (\text{degenerate with }^2A_2) \qquad (2) \\ &^2A_2\ (\mathrm{d}\sigma)^1(\mathrm{d}\pi)^1(\mathrm{d}\delta)^1(\mathrm{d}\bar{\delta})^2(\mathrm{d}\bar{\pi})^2 \end{aligned}$$

Although all three configurations are d^7 Ru^+, they have different electron repulsion energies (even when the orbital shapes are identical), and we see by examination of (2) that it is this *atomic–electron repulsion energy* that *determines the relative energies* in (1). For example, $^2B_2$ has four electrons in the xy plane ($\delta^2\bar{\delta}^2$), whereas $^2A_1$ and $^2A_2$ have the doubly occupied orbitals in different planes ($\bar{\delta}^2\bar{\pi}^2$ or $\delta^2\bar{\pi}^2$), leading to lower electron repulsion. Thus, in predicting the ground configuration of $RuCH_2^+$ we need only consider two factors:

(i) which states of Ru^+ can form two covalent bonds, and

(ii) of the states satisfying (i), which occupation of the nonbonding d orbitals has the lowest atomic energy (lowest electron repulsion).

B. Bonding in the Ground State, $RuCH_2^+$ ($^2A_2$). The generalized valence bond (GVB) one-electron orbitals for the Ru–C σ and π bonds are shown in Figure 1 where we see that both bonds are quite covalent. The Ru–C σ bond pair has an overlap of 0.68, with 1.04 electrons ascribed to Ru^+ and 0.96 electron associated with CH_2.[9] The Ru–C π bond pair has an overlap of 0.48, with 1.16 electrons localized on Ru^+ and the other 0.84 electron on CH_2. The bonding orbitals on Ru are almost entirely 4d in character (the Ru σ bonding orbital is 87.8% 4d and 12.2% 5sp, while the Ru π bonding orbital is 99.1% 4d and 0.9% 5p). Thus the $RuCH_2^+$ complex is best described as d^7 Ru^+, forming a covalent double bond with triplet methylene.

The covalent nature of the $Ru{=}CH_2$ bond is further supported by comparison with the bonds in ethylene. The GVB orbitals for the σ and π bonds of $CH_2{=}CH_2$ are shown in Figure 1, where it is evident that the carbon σ and π character in both $RuCH_2^+$ and $CH_2{=}CH_2$ are very similar. The C–C σ overlap in ethylene is 0.88, while the C–C π bond overlap is 0.65. The overlaps are lower in $RuCH_2^+$ due to the longer bond lengths [$R(Ru{=}C) = 1.88$ Å vs. $R(C{=}C) = 1.34$ Å;[10] see Figure 2] and some mismatch in orbital extent for Ru 4d vs. C 2sp. However, the trends in overlap (σ vs. π) compare well: $S_\sigma - S_\pi = 0.23$ for $CH_2{=}CH_2$ and $S_\sigma - S_\pi = 0.20$ for $RuCH_2^+$ ($^2A_2$).

One further indication of covalent bonding becomes evident as we pull the molecule apart, breaking the double bond. For covalent bonds, the overlap in each bond decreases monotonically as the bond length is increased from its equilibrium position, and this is indeed observed for $RuCH_2^+$ ($^2A_2$) (see Figure 3). The opposite behavior of the bond pair overlap observed for the low-lying $^4A_2$ excited state of $RuCH_2^+$ will be discussed in section III.

C. Oxidation-State Formalisms. The result of a *covalent* double bond between a metal atom and CH_2 is in *direct contradiction* with the literal interpretation of the popular oxidation-state formalism, which denotes the methylidene ligand as CH_2^{2-} when bound to transition metals. The oxidation formalism *implies ionic bonding*; our theoretical results show clearly that bonds between transition metals and CH_2 are often *covalent*, not ionic.

From these and other GVB calculations, the following alternatives formalism has evolved:

(1) Consider every ligand as neutral and start with the appropriate charge state of the metal (Ti^0 for **3**, Cr^0 for **4**, Mo^0 for

---

(8) (a) Fischer, E. O.; Dötz, K. H. *Chem. Ber.* **1970**, *103*, 1273. (b) Dötz, K. H.; Fischer, E. O. *Ibid.* **1972**, *1356*. (c) Stevens, A. E.; Beauchamp, J. L. *J. Am. Chem. Soc.* **1979**, *101*, 6449. (d) Brandt, S.; Helquist, P. J. *Ibid.* **1979**, *101*, 6473. (e) Brookhart, M.; Humphrey, M. B.; Katzer, H. J.; Nelson, G. O. *Ibid.* **1980**, *102*, 7803. (f) Brookhart, M.; Tucker, J. R.; Husk, G. R. *Ibid.* **1981**, *103*, 979. (g) Casey, C. P.; Vollendorf, N. W.; Haller, K. J. *Ibid.* **1984**, *106*, 3754. (h) Casey, C. P.; Shusterman, A. J. *Organometallics* **1985**, *4*, 736. (i) Brookhart, M.; Studabaker, W. B.; Husk, G. R. *Ibid.* **1985**, *4*, 943. (j) Casey, C. P.; Miles, W. H.; Tukada, H. *J. Am. Chem. Soc.* **1985**, *107*, 2924. (k) Stevens, A. E.; Beauchamp, J. L. *Ibid.* **1978**, *100*, 2584.

(9) The electron populations and hybrid character are determined by summing the Mulliken populations from both natural orbitals (weighted by occupation) of each GVB bond pair.

(10) Harmony, M. D.; Laurie, V. W.; Kuczkowski, R. L.; Schwendeman, R. H.; Ramsay, D. A.; Lovas, F. J.; Lafferty, W. J.; Maki, A. G. *J. Phys. Chem. Ref. Data* **1979**, *8*, 676.

Table I. Single Configuration SCF and CI Energies for d^7 Ru^+

relevant $RuCH_2^+$ symmetry[a]	Ru^+ hole config[b]			Ru^+ full config					Ru^+ SCF total energy, hartrees	Ru^+ $H(i,i)$[c] total energy, hartrees	ΔE(SCF),[d] kcal/mol	ΔE(CI),[e] kcal/mol
				σ	π	$\bar{\pi}$	δ	$\bar{\delta}$				
$^2B_2$	σ	π	$\bar{\pi}$	1	1	1	2	2	-4437.14079	-4437.13959	+26.8	+27.4
-	$\bar{\pi}$	δ	$\bar{\delta}$	2	2	1	1	1		-4437.15049		+20.5
-	π	δ	$\bar{\delta}$	2	1	2	1	1	-4437.15145	-4437.15049	+20.1	+20.5
$^4A_2$	σ	δ	$\bar{\delta}$	1	2	2	1	1	-4437.17283	-4437.17229	+6.7	+6.8
$^4B_2$	σ	$\bar{\pi}$	$\bar{\delta}$	1	2	1	2	1	-4437.17282	-4437.17229	+6.7	+6.8
$^2A_1$, $^4B_1$[f]	σ	π	$\bar{\delta}$	1	1	2	2	1	-4437.17282	-4437.17229	+6.7	+6.8
$^4B_1$	σ	$\bar{\pi}$	δ	1	2	1	1	2	-4437.17282	-4437.17229	+6.7	+6.8
$^2A_2$	σ	π	δ	1	1	2	1	2	-4437.17282	-4437.17229	+6.7	+6.8
-	π	$\bar{\pi}$	$\bar{\delta}$	2	1	1	2	1		-4437.18319		0.0
-	π	$\bar{\pi}$	δ	2	1	1	1	2	-4437.18354	-4437.18319	0.0	0.0

[a] The C_{2v} symmetries listed for $RuCH_2^+$ doublet states correspond to $^3B_1$ CH_2 bound to the configuration of Ru^+ listed in the next column. The quartet states of $RuCH_2^+$ correspond to $^1A_1$ CH_2 bound to the configuration of Ru^+ listed in the next column. [b] The doubly occupied orbitals have been omitted for clarity in discussions. Our convention for d-orbital symmetries has $\sigma = 4d_{z^2}$, $\pi = 4d_{xz}$, $\bar{\pi} = 4d_{yz}$, $\delta = 4d_{xy}$, $\bar{\delta} = 4d_{x^2-y^2}$, where the Ru–C axis is z and the $RuCH_2^+$ plane is yz. Thus, π and δ are "pi-like" (antisymmetric) with respect to the molecular plane. [c] Using field-averaged orbitals from the SCF wave function ($^7/_5$ electrons per d orbital to obtain equivalently shaped d orbitals), we constructed all 10 states corresponding to the d^7 configuration of Ru^+. A 10-configuration CI leads to seven states corresponding to ^4F (each with total energy -4437.183 19 hartrees) and three states corresponding to ^4P (higher by 34.2 kcal/mol). When real orbitals are used, only two of these 10 configurations ($\pi\bar{\pi}\delta$) and ($\pi\bar{\pi}\bar{\delta}$) have pure ^4F symmetry and none has pure ^4P symmetry. The diagonal energies for these configurations are given by $H(i, i)$. For some configurations we solved for the SCF wave function (rather than using field-averaged orbitals); this leads to energies lower by 0.1–0.6 kcal. The energy differences in $H(i, i)$ are a measure of the increased electron repulsion energy (exchange energies) in these states. [d] SCF excitation energy (in kcal/mol) from the $\pi\bar{\pi}\delta$ ground state of Ru^+. [e] CI excitation energy (in kcal/mol) from the $\pi\bar{\pi}\delta$ ground state of Ru^+. [f] $RuCH_2^+$ ($^4B_1$) excited state with a single σ-donor bond.

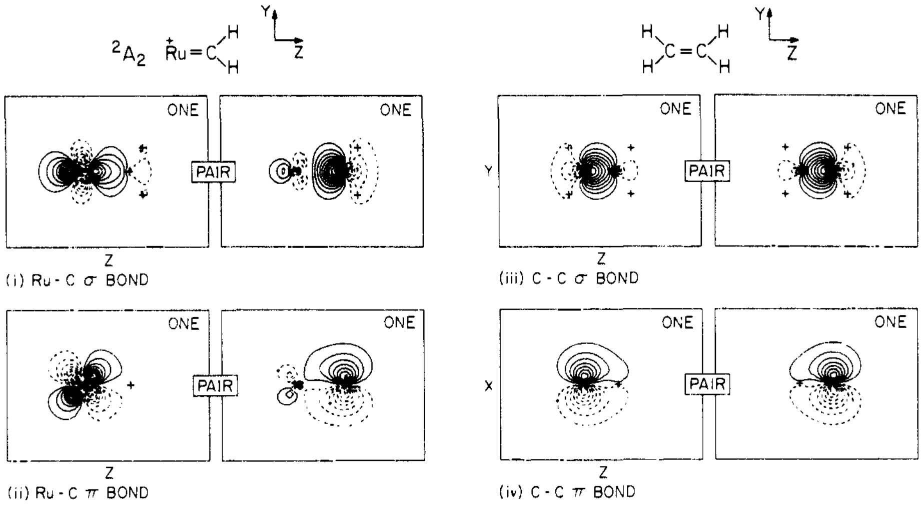

Figure 1. GVB orbitals for the methylidene complex $RuCH_2^+$ ($^2A_2$) [(i) and (ii)] and for $CH_2{=}CH_2$ [(iii) and (iv)]. (i) Ru–C σ bond; (ii) Ru–C π bond; (iii) C–C σ bond; (iv) C–C π bond. Contours reflect regions of constant amplitude ranging from -0.5 to +0.5 a.u., with increments of 0.05 a.u.

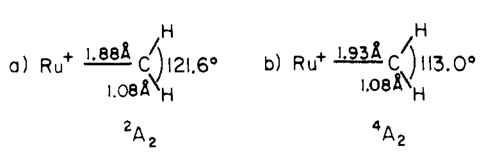

Figure 2. Optimum geometries at the GVB(2/4)-RCI level for (a) ground-state $RuCH_2^+$ ($^2A_2$) and (b) excited-state $RuCH_2^+$ ($^4A_2$).

5, and Ru^+ for **13**), and consider first the ground atomic configuration for the metal (s^2d^2 for Ti, s^1d^5 for Cr and Mo, and d^7 for Ru^+).

(2) Ligands such as cyclopentadienyl (Cp) or Cl prefer larger amounts of ionic character in the bond and consequently prefer to bond to s-like metal orbitals rather than d orbitals (lower ionization potential (IP) for s than d and hence easier charge transfer). For a qualitative analysis it is just as well to consider these ligands as reduced (e.g., Cp^- or Cl^-) and the metal oxidized. For two such electronegative ligands to both obtain partial ionic bonds requires an s^2 metal configuration. In the GVB description, an s^2 pair is described by (s + pz) and (s − pz) hybrid orbitals, and each plays the role of bonding to one electronegative ligand (thus preferring a 180° bond angle). If there are more than two such electronegative ligands, the ionic bonds must involve metal d electrons (since s^3 is not allowed and s^2p is generally quite high) and consequently the bonds become less ionic.

(3) Bonds to alkyl, aryl, and hydride ligands prefer covalent bonding, particularly if the metal has enough electronegative ligands to utilize the s electrons on the metal.

(4) More subtle effects can be involved for groups with active p-like lone pairs such as oxo or alkoxide groups, but we will eschew them here.

Although more cumbersome than the usual oxidation-state formalism, we find that this VB formalism provides a simple means of correctly predicting the character of numerous quite different states of organometallic complexes. Some examples follow:

(1) For $RuCH_2^+$ we label the Ru atom as Ru(I) and consider the ground d^7 configuration, since the bonds are covalent and there is a +1 charge on the metal.

(2) Since neutral Ru atom has an s^1d^7 ground state and Cl is very electronegative, we expect RuCl to have a very ionic bond,[11] and hence the Ru in RuCl is labeled as Ru(I). Further, ligands added to Ru^ICl should form covalent bonds, since all remaining unpaired Ru electrons are in d orbitals, as in $Ru^I{=}CH_2^+$.

(3) GVB calculations on $ClRu(H)(CH_2)$[12] show the metal to have the same electronic character as in $Ru^I{=}CH_2^+$; namely, the

---

[11] Carter, E. A.; Goddard, W. A., III, unpublished.

[12] Carter, E. A.; Goddard, W. A., III, manuscript in preparation.

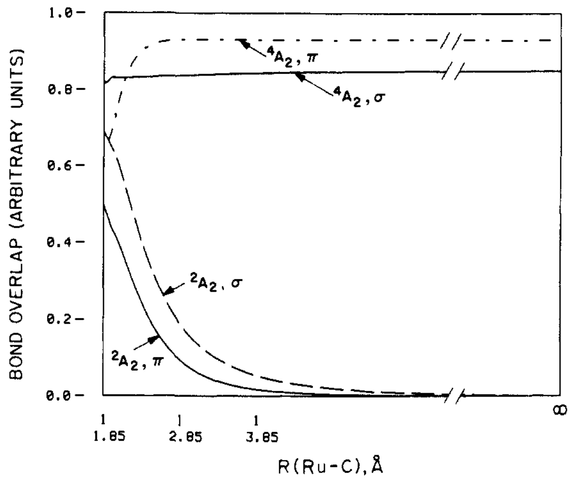

Figure 3. Ru-C σ and π bond overlaps for the $^4A_2$ (donor-acceptor or carbene-like bond) and $^2A_2$ (covalent or methylidene-like bond) states of RuCH$_2^+$ as a function of distance. Overlap decreases with distance for covalent bonds but is approximately constant for donor-acceptor bonds.

bonds to H and CH$_2$ are quite covalent and the CH$_2$ bonds in both Ru(I) systems are nearly identical in character. **14** depicts the electronic character at Ru(I) as three covalent bonds drawn as lines, one dative bond from Cl$^-$ as an arrow, and two doubly occupied d orbitals by two pairs of dots.

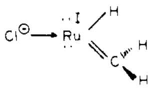

14

(4) (Cl)(NO)(PPh$_3$)$_2$Os(CH$_2$)[13] is written as

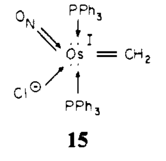

15

indicating that the metal is thought of as a d^7 Os(I) (after making an ionic bond to Cl to form Cl$^-$) with three covalent d bonds (two to CH$_2$ and one to the π orbital of NO), leaving two double occupied d orbitals. In addition to the five d orbitals of Os(I), the four arrows indicate the ligands overlapping the four empty Os 6s and 6p orbitals to yield a total of 18 electrons associated with the metal (four in doubly occupied d orbitals, six in three covalent metal-ligand bonds, and eight in the pairs indicated with arrows).

(5) (Cp*)(NO)(PPh$_3$)Re(CH$_2$)$^+$[14] is written as

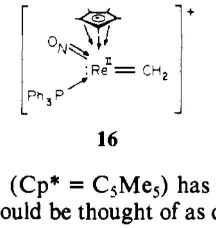

16

to show that the Cp* (Cp* = C$_5$Me$_5$) has formed an ionic bond and thus the metal should be thought of as d^5 Re(II). In this case there are five ligand-to-metal donor bonds, requiring an empty 5d orbital in addition to the four empty 6s and 6p orbitals, so that the d^5 configuration of Re(II) has one doubly occupied d orbital plus three singly occupied d orbitals (which are used in the three covalent bonds).

Examples 1-5 illustrate how to designate and predict the character of metal-ligand bonds, the nonbonding electron configuration at the metal, and the overall degree of saturation of the metal complex. This new VB oxidation-state formalism provides logical explanations and predictions for bond character trends in the forthcoming sections.

Table II. Vibrational Frequencies (cm^{-1}) for the $^2A_2$ and $^4A_2$ States of RuCH$_2^{+a}$

state	$\nu_{\text{Ru-C}}$	$\nu_{\text{C-H}}$	$\nu_{\text{HCHscissors}}$
$^2A_2$	665	3245	1461
$^4A_2$	464	3256	1437

^{a} Based on ω_e from cubic spline fits to results from GVB(2/4)-RCI calculations.

D. Geometries. The optimum calculated geometry for RuCH$_2^+$ ($^2A_2$) is shown in Figure 2a. The Ru-C bond length of 1.88 Å may be compared with experimental values for metal-methylidene bond lengths such as R(Os^I=CH$_2$) = 1.92 Å in **15**[13] and R(Re^{II}=CH$_2$) = 1.898 Å in **16**.[14] The Ru^I-C bond length is expected to be shorter than the Os^I-C bond length since the d-orbital extent for Ru(I) is smaller than that for Os(I) (4d for Ru vs. 5d for Os). For d^5 Re(II), the greater orbital extent due to a higher n quantum number is nearly canceled by the higher effective nuclear charge, which causes a greater contraction of the orbitals for Re(II) than for Ru(I). Consistent with our expectations, covalent d bonds involving d orbitals of similar size result in very similar bond lengths.

The other geometrical parameters of RuCH$_2^+$ are not unusual. The C-H bond lengths (1.08 Å) are typical for sp^2 C-H bonds. The HCH bond angle of 121.6° is characteristic of a triplet methylene forming two covalent bonds to another moiety (a metal or another CH$_2$). For instance, CrCH$_2^+$ ($^4B_1$) has θ(HCH) = 117.6° and CH$_2$=CH$_2$ has θ(HCH) = 117.6°.[1,10] On the other hand, θ(HCH) = 133° for free CH$_2$ ($^3B_1$),[15] indicating that electron pair-pair repulsions decrease θ(HCH) upon complexation.

E. Vibrational Frequencies. The vibrational frequencies for RuCH$_2^+$ ($^2A_2$) are shown in Table II. The Ru-CH$_2$ stretching frequency is 665 cm^{-1}, which may be compared with theoretical values for CrCH$_2^+$ ($^4B_1$) of $\nu_{\text{Cr-C}}$ = 542 cm^{-1} and the values obtained for two rotamers of ClRu^{I}H(CH$_2$) of $\nu_{\text{Ru-C}}$ = 746 and 798 cm^{-1}.[1,12] The M=C frequencies correlate well with bond strength in order of Cr$^+$ < Ru$^+$ < ClRuH. The D_e(M^I=CH$_2$) are 44.0, 68.0 (vide infra), and 85.5 kcal/mol for M = Cr$^+$, Ru$^+$, and ClRuH, respectively. A recent matrix isolation study[16] on FeCH$_2$ provides the first experimental M-CH$_2$ stretching frequency, 623.6 cm^{-1}, in good agreement with our value for RuCH$_2^+$. The C-H symmetric stretch at 3245 cm^{-1} and the HCH scissors mode at 1461 cm^{-1} are in reasonable agreement with those expected for sp^2 C-H bonds. (The corresponding values in CH$_2$=CH$_2$ are 3056 and 1393 cm^{-1}, respectively.[17])

F. The Ru=C Bond Strength in RuCH$_2^+$ ($^2A_2$). Few metal-ligand bond strengths for saturated organometallic complexes are known, either experimentally or theoretically. The majority of those that have been measured are for gas-phase, highly unsaturated bare metal cations with just one ligand.[18] In this section we will consider the relationship expected between the bond energies in such unsaturated species as compared with saturated organometallic complexes.

All calculations carried out on RuCH$_2^+$ are such that the wave function for RuCH$_2^+$ at its equilibrium geometry (given in Figure 2a) dissociates smoothly to the appropriate covalent fragments, retaining the same level of electron correlation in the fragments as that included for the complex. In addition, we allow the fragments to relax to their equilibrium geometries, thus obtaining

---

(13) Hill, A. F.; Roper, W. R.; Waters, J. M.; Wright, A. H. *J. Am. Chem. Soc.* **1983**, *105*, 5939.

(14) Patton, A. T.; Strause, C. E.; Kuobler, C. B.; Gladysz, J. A. *J. Am. Chem. Soc.* **1983**, *105*, 5804.

(15) Shih, S.-K.; Peyerimhoff, S. D.; Buenker, R. J.; Peric, M. *Chem. Phys. Lett.* **1978**, *55*, 206.

(16) Chang, S.-C.; Kafafi, Z. H.; Hauge, R. H.; Billups, W. E.; Margrave, J. L. *J. Am. Chem. Soc.* **1985**, *107*, 1447.

(17) Shimanouchi, T. *Tables of Molecular Vibrational Frequencies*; U. S. Government Printing Office: Washington, DC, 1972, NSRDS-NBS-92.

(18) See, for example, (a) Armentrout, P. B.; Beauchamp, J. L. *J. Am. Chem. Soc.* **1981**, *103*, 784. (b) Armentrout, P. B.; Halle, L. F.; Beauchamp, J. L. *Ibid.* **1981**, *103*, 6501. (c) Mandich, M. L.; Halle, L. F.; Beauchamp, J. L. *Ibid.* **1984**, *106*, 4403.

Table III. Bond Dissociation Energies (kcal/mol) for the Methylidene State of $RuCH_2^+$ ($^2A_2$)

calculational level[a]	D_e(Ru=C)	$RuCH_2^+$($^2A_2$) total energy, hartrees[b]	fragment total energies, hartrees: Ru^+	fragment total energies, hartrees: CH_2($^3B_1$)
HF	−11.5	−4476.088 67 (1/1)	−4437.183 54 (1/1)	−38.923 41 (1/1)
GVB(2/4)-PP	27.6	−4476.151 00 (4/4)	−4437.183 54 (1/1)	−38.923 41 (1/1)
RCI(2/4)	45.4	−4476.179 23 (9/17)	−4437.183 54 (1/1)	−38.923 41 (1/1)
$RCI_\pi*D_\sigma + RCI_\sigma*D_\pi$	55.2	−4476.194 88 (989/2627)	−4437.183 54 (1/1)	−38.923 41 (1/1)
$(RCI(2/4)*S)_{val,Ru}$	59.5	−4476.202 74 (321/1233)	−4437.184 49 (21/48)	−38.923 41 (1/1)
$(RCI(2/4)*S)_{val,full}$	63.3	−4476.220 28 (507/2091)	−4437.184 49 (21/48)	−38.934 99 (22/44)
$RCI_\pi*D_\sigma + RCI_\sigma*D_\pi + (RCI(2/4)*S)_{val,full}$	68.0	−4476.227 77 (1379/4377)	−4437.184 49 (21/48)	−38.934 99 (22/44)

[a] Each of these calculations is explained in detail in section V. [b] The number of spatial configurations/number of spin eigenfunctions are given in parentheses.

the adiabatic, dissociation-consistent[19] bond energy.

The Ru=C bond energies for $RuCH_2^+$ ($^2A_2$) as a function of electron correlation are shown in Table III. At the highest level, we find a direct, adiabatic Ru=C bond energy of D_e = 68.0 kcal/mol, for $RuCH_2^+$ ($^2A_2$) dissociating into ground-state fragments Ru^+ (^4F) ($\pi\bar{\pi}\delta$ and $\pi\bar{\pi}\bar{\delta}$ in Table I) and CH_2 ($^3B_1$). Note that although the metal is in a promoted state at R_e (6.7 kcal/mol above ^4F; see Table I), the metal relaxes to ^4F Ru^+ as the bond breaks.[20] This direct bond energy is expected to be a lower limit since electron-correlation effects increase when more electrons are in the same regions of space. Analogous calculations for the double bond of $CH_2=CH_2$ (using the same basis sets and level of CI as in $RuCH_2^+$) lead to a calculated bond energy of 174.4 kcal/mol,[1] which is 5.6 kcal/mol smaller than the experimental value of $D_e(CH_2=CH_2)$ = 180.0.[21] We expect the residual correlation error in $Ru=CH_2^+$ to be at least as high as in $CH_2=CH_2$ (due to the presence of the other valence d electrons on Ru); hence, we estimate the exact bond energy for $RuCH_2^+$ ($^2A_2$) to be

$$D_e^{\text{exact}}(Ru^+=CH_2) = 73.6 \text{ kcal/mol}$$

G. Correlation between Saturated and Unsaturated M=CH₂ Bond Energies. Since gas-phase $RuCH_2^+$ has not yet been observed, a direct comparison cannot be made with experiment. However, we have carried out equivalent calculations on the larger $Ru^I=CH_2$ complex, $ClRu^IH(CH_2)$, **14**, which in the $^1A'$ state should model coordinatively saturated, 18-electron ruthenium-alkylidene complexes such as $CpRu^I(L)(R)(CH_2)$ (where L = CO or PR_3 and R = alkyl, aryl, or H), which has been postulated as an intermediate in the isomerization of a dimethylruthenium complex to an olefin hydride complex.[22] For **14**, at the same level of electron correlation and the same basis sets as used in the present study, we find a direct, adiabatic Ru=C bond energy of D_e(Ru=C) = 85.5 kcal/mol (vs. 68.0 for $RuCH_2^+$).[12]

Why is the bond stronger in the more highly saturated system even though the metal–carbon bond has not changed character? The answer involves the change in spin coupling necessarily associated with covalent-bond formation. For atoms, the ground state has the singly occupied orbitals coupled to form the highest spin state (Hund's rule). This results from the exchange energy terms

$$E^{\text{ex}} = -\sum_{i>j} K_{i\alpha j\alpha} - \sum_{i>j} K_{i\beta j\beta}$$

which arise (from the Pauli principle) *only* for orbitals with the same spin. For d^7 Ru^+, the quartet state ($S = {}^3/_2$) with five α spins and two β spins leads to 11 exchange interactions, each of which contributes an average of negative 15 kcal/mol to the energy.[23] In contrast, the atomic doublet state ($S = {}^1/_2$) with four α spins and three β spins leads to only nine exchange interactions and an energy about 30 kcal/mol higher. However, formation of a covalent bond (perfect pairing) between a ligand and a singly occupied d orbital necessarily requires that the bond pair be coupled into a singlet (low-spin) with the result that the metal d orbital is half the time α and half the time β. This results in a decrease in atomic exchange stabilization that goes hand in hand with covalent bonding to singly occupied d orbitals. The magnitude of this effect increases with the number of other singly occupied high-spin-paired d orbitals and hence it depends on how saturated the bonding to the metal is.

In forming a covalent double bond to CH_2 in (singlet) $ClRu(CH_2)H$, the two metal orbitals that were originally high-spin ($\alpha\alpha$, leading to a $-K_{dd}$ exchange term) in the (triplet) ClRuH fragment must now each become α half the time and β half the time, with the result that they have the same spin only half the time (i.e., $\alpha\alpha + \alpha\beta + \beta\alpha + \beta\beta$ leads to a $-{}^1/_2K_{dd}$ average exchange term). The result is that the atomic exchange energy becomes less negative by ${}^1/_2K_{dd}$ = 7.5 kcal/mol. Thus

$$D_e[(Cl)(H)Ru=CH_2] = D_{int}(Ru=CH_2) - 7.5 \text{ kcal/mol}$$

where $D_{int}(Ru=CH_2)$ is the intrinsic (exchangeless) metal–methylene bond strength (for any $RuCH_2$ system). If there is a third unpaired d orbital on the metal (as in Ru^+), the spin of the free atom is $\alpha\alpha\alpha$, leading to $-3K_{dd}$ among those three electrons, but after bonding to two of the d orbitals, the spins on the metal are $\alpha\alpha\alpha + \alpha\beta\alpha + \beta\alpha\alpha + \beta\beta\alpha$, leading to an average of (1/4)(3 + 1 + 1 + 1) = $3/2K_{dd}$. Thus, in $RuCH_2^+$, the $M=CH_2$ bond loses $3/2K_{dd}$ = 22.5 kcal/mol. Thus

$$D_e(Ru^+=CH_2) = D_{int}(Ru=CH_2) - 22.5 \text{ kcal/mol}$$

and we expect

$$D_e[(Cl)(H)Ru=CH_2] - D_e(Ru^+=CH_2) = 15 \text{ kcal/mol} \quad (3)$$

Indeed, from the calculated bond energies (85.5 and 68.0), we obtain 17.5 kcal/mol for the quantity in (3). Thus *the differences in bond strengths for saturated vs. unsaturated metal complexes are dominated by the differential loss of exchange coupling on the metal.* Hence, we obtain

$$D_{int}(Ru=CH_2) = 68.0 + 22.5 = 90.5 \text{ kcal/mol} \quad (4)$$

$$D_{sat}(Ru=CH_2) = D_{int} - {}^1/_2K_{dd} = 83.0 \text{ kcal/mol} \quad (5)$$

---

(19) Bair, R. A.; Goddard, W. A., III, submitted for publication in *J. Phys. Chem.*

(20) At R_e, $RuCH_2^+$ ($^2A_2$) has the Ru^+ configuration $\sigma^1{}_{z^2}\pi^1{}_{xz}\bar{\pi}^2{}_{yz}\bar{\delta}^2{}_{x^2-y^2}\delta^1{}_{xy}$, which, under C_{2v} symmetry, relaxes as the bond breaks by mixing d_{z^2} and $d_{x^2-y^2}$ to form $\sigma^1{}_{z^2-y^2}\pi^1{}_{xz}\bar{\pi}^2{}_{yz}\bar{\delta}^2{}_{2x^2-y^2-z^2}\delta_{xy}{}^1$. This latter configuration has ^4F symmetry with respect to the x axis.

(21) *JANAF Thermochemical Tables*; U.S. Government Printing Office: Washington, DC, 1970, NSRDS-NBS-37.

(22) Kletzin, H.; Werner, H.; Serhadli, O.; Ziegler, M. L. *Angew. Chem., Int. Ed. Engl.* **1983**, *22*, 46.

(23) K_{dd} = average exchange energy between two d orbitals. $K_{dd}(Ru^+)$ = 15 kcal/mol and K_{sd} = 7.5 kcal/mol from our ab initio Hartree-Fock calculations on Ru^+.

(where D_{sat} is the bond energy expected for a saturated Ru=CH$_2$ complex) from our direct GVB calculations. Including the estimated correction of 5.6 kcal/mol, (4) and (5) become

$$D_{\text{int}}^{\text{exact}}(\text{Ru}{=}\text{CH}_2) = 96.1 \text{ kcal/mol} \quad (6)$$

$$D_{\text{sat}}^{\text{exact}}(\text{Ru}{=}\text{CH}_2) = 88.6 \text{ kcal/mol} \quad (7)$$

We expect $D_{\text{int}}(\text{Ru}{=}\text{CH}_2)$ to remain fairly constant, regardless of the nature or existence of ancillary ligands, for a given electronic state of the metal atom. This is borne out in the cases above, RuCH_2^+ and ClRuH(CH$_2$), for which D_{int} = 90.5 and 93.0 kcal/mol, respectively.

To see how to use these quantities for predicting bond energies, consider the 18-electron complex, Cp(dppe)Ru=CH$_2^+$ (the Fe analogue is known[24]): Ru(II) is d^6, but this complex requires

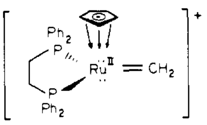

five empty acceptor orbitals (the 5s, three 5p, and one 4d) on the metal (as indicated by the arrows). The requirement of a d hole plus two singly occupied d's that can bond to CH$_2$ forces the other four electrons to occupy the two remaining d orbitals, leading to the intermediate triplet spin state of Ru(II). Thus, in bonding CH$_2$ to the fragment Cp(dppe)Ru$^+$, the two unpaired electrons in the intermediate spin state lose $^1/_2K_{\text{dd}}$, and we predict a bond energy of

$$D_e^{\text{exact}}[\text{Cp(dppe)Ru}{=}\text{CH}_2^+] = D_{\text{int}}(\text{Ru}{=}\text{CH}_2) - 7.5 = 96.1 - 7.5 = 88.6 \text{ kcal/mol}$$

In contrast, removal of the chelating phosphine should lower the bond energy, since CpRu=CH$_2^+$, does not require a d hole for

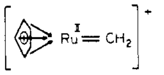

donation from the Cp$^-$ ligand, leading to a high-spin d^6 Ru(II). In this case, the fragment CpRu$^+$ has four unpaired spins with $-6K_{\text{dd}}$ between them, while CpRuCH$_2^+$ with two unpaired electrons has only $-3^1/_2K_{\text{dd}}$ involving these four electrons (after forming the bond). Therefore, we expect

$$D_e^{\text{exact}}(\text{CpRu}^+{=}\text{CH}_2) = 96.1 - (5/2)(15) = 58.6 \text{ kcal/mol}$$

Thus, dramatic differences in bond energies are expected bewteen unsaturated vs. saturated complexes, *even as the nature of the bond being broken remains constant.*

This leads to the exchange moderated ligand effect: Added ligands serve to quench many of the intraatomic exchange terms (due either to covalent bond formation or to coordinated Lewis bases forcing the metal into a lower spin state). The differential-exchange energy lost in the more saturated complex will be less than that lost in a highly unsaturated system, leading to a larger observed Ru=CH$_2$ bond energy.

As another example, consider the saturated system (Cl)(NO)Ru$^{\text{I}}$(PPh$_3$)$_2$=CH$_2$. Although RuCH$_2^+$ has an estimated Ru-C bond energy of 73.6 kcal/mol, here we expect to have an Ru-C bond energy of 96.1 − $^1/_2K_{\text{dd}}$ = 88.6 kcal/mol, the same as predicted for our model compound ClRuH(CH$_2$) and for Cp(dppe)Ru=CH$_2^+$. Thus, *saturated metal complexes are expected to have substantially larger bond energies than those of their unsaturated counterparts.*

This result suggests two further extensions. First, the fact that the intrinsic bond strengths of these two ruthenium(I)-alkylidene systems are essentially identical implies that the character of the bonding is also the same for both systems. Thus, by understanding the simple case of RuCH$_2^+$, we can understand the bonding in the larger Ru(I) complex, ClRuH(CH$_2$), and in other electronically analogous systems. Second, the simplicity (and generality) of the expression for the intrinsic bond strength is provocative; it suggests that we may be able to estimate the bond energies of saturated organometallic (or any other) complexes from bond energies known for unsaturated complexes containing the same ligand. Calculation of $D_{\text{int}} = D_e(\text{unsaturated}) + \Delta K_{\text{dd}}$ yields

$$D_e(\text{saturated}) = D_e(\text{unsaturated}) + \Delta K_{\text{dd}} - {}^1\!/_2K_{\text{dd}}$$

assuming covalent bonds to d orbitals are formed in the saturated complex. (This does require that the metal atoms have the same electronic state in both complexes.)

H. **Summary.** We see that each property of the $^2A_2$ state of RuCH$_2^+$ taken separately or together, implicates one possible description of the bonding between Ru$^+$ and CH$_2$. Thus, we may best think of this complex as consisting of high-spin d^7 Ru$^+$ forming two covalent bonds to $^3B_1$ CH$_2$.

III. A Low-Lying Excited State of RuCH$_2^+$: Carbene Bonding

A. Covalent vs. Donor-Acceptor Bonding. As discussed in section II.G, the intraatomic exchange stabilization of a free metal ion necessarily weakens metal-ligand bonds, since this stabilization is at least partially quenched upon complexation. In section II, we examined the lowest spin state of RuCH$_2^+$, formed from ground-state fragments, and found a $^2A_2$ ground state. However, higher spin states may be important if they lead to less exchange energy quenching in the complex. Thus we investigated the possible existence of low-lying quartet states of RuCH$_2^+$.

There are three ways in which quartet states may be formed for RuCH$_2^+$. First, we can form a quartet state directly from the ground $^2A_2$ state by triplet-coupling the weakest bond, namely, the π bond. This leads to a singly bonded $^4A_2$ state of Ru$^+$-CH$_2$, which suffers less exchange loss than the doublet ground state (only 1 K_{dd} = 15 kcal/mol), but it is destabilized by forcing the overlapping Ru dπ orbital and the C pπ orbital to be orthogonal. The $^4A_2$ state formed in this manner lies above the $^2A_2$ ground state by 50.9 kcal/mol.

A second way to form a quartet state of RuCH$_2^+$ is to promote d^7 Ru$^+$ to s^{1}d^6 before bonding to triplet CH$_2$. This costs 28.4 kcal/mol,[25] but in return we can form two covalent bonds to CH$_2$, thus avoiding the π repulsions which caused the above quartet to fail.

Promoting Ru$^+$ to the s^{1}d^6 excited state leads to five equivalent states (the ^{6}D state). When the same labeling scheme as in section II.A (the corresponding RuCH$_2^+$ symmetries are shown in parentheses) is used, these become

$$\underline{(5s)}^1(d\sigma)^2\underline{(d\pi)}^1(d\bar{\pi})^1(d\delta)^1(d\bar{\delta})^1 \quad (^4B_1)$$

$$(5s)^1(d\sigma)^1(d\pi)^2(d\bar{\pi})^1(d\delta)^1(d\bar{\delta})^1 \quad (^6A_1)$$

$$(5s)^1\underline{(d\sigma)}^1\underline{(d\bar{\pi})}^1(d\pi)^2(d\delta)^1(d\bar{\delta})^1 \quad (^4A_2)$$

$$(5s)^1\underline{(d\sigma)}^1\underline{(d\pi)}^1(d\bar{\pi})^1(d\delta)^2(d\bar{\delta})^1 \quad (^4B_2)$$

$$(5s)^1\underline{(d\sigma)}^1\underline{(d\pi)}^1(d\bar{\pi})^1(d\delta)^1(d\bar{\delta})^2 \quad (^4B_1)$$

Bringing up the CH$_2$ in the *yz* plane, we can form a double bond involving 4dσ and 4dπ orbitals for the last three ($^4A_2$, $^4B_2$, and $^4B_1$), and we can form a double bond involving 5s and 4dπ for the last three and the first (also $^4B_1$). Thus we expect three nearly degenerate, doubly bonded quartet states (symmetries $^4A_2$, $^4B_2$, and $^4B_1$) to arise from binding Ru$^+$ (s^{1}d^6) to CH$_2$ ($^3B_1$). The σ bond is allowed to be either s- or d-like on the metal.

In addition to the promotional energy (d^7 → s^{1}d^6), we must also consider the loss of intraatomic exchange interactions for s^{1}d^6 Ru$^+$ in order to fully assess the energetics of complexation. Assuming pure dσ and pure dπ orbitals are utilized on the metal, forming

---

[24] Brookhart, M.; Tucker, J. R.; Flood, T. C.; Jensen, J. *J. Am. Chem. Soc.* **1980**, *102*, 1203.

[25] Our calculations at the HF level lead to $E_p(^4F \rightarrow {}^6D)$ = 28.4 kcal/mol, while the experimental E_p = 25.1 kcal/mol averaged over angular momentum states (E_p = promotional energy). Moore, C. E. *Atomic Energy Levels*; NSRDS-NBS-35, 1971, Vol. 3, p 25.

Table IV. Comparison of Related State Splittings in $RuCH_2^+$ and Ru^{+}[a]

	$RuCH_2^+$		corresponding Ru^+ states				
state	total energy, hartrees	excitation energy, kcal/mol	hole config			$H(i, i)$, hartrees	excitation energy, kcal/mol
$^4B_1$	−4476.163 98	+9.6	σ	$\bar{\pi}$	δ	−4437.172 29	0.0
$^4B_2$	−4476.164 13	+9.5	σ	$\bar{\pi}$	$\bar{\delta}$	−4437.172 29	+0.0
$^4A_2$	−4476.164 19	+9.4	σ	δ	$\bar{\delta}$	−4437.172 29	+0.0
$^2B_2$	−4476.147 38	+20.0	σ	π	$\bar{\pi}$	−4437.139 59	+20.6
$^2A_1$	−4476.177 31	+1.2	σ	π	$\bar{\delta}$	−4437.172 29	+0.0
$^2A_2$	−4476.179 23	0.0	σ	π	δ	−4437.172 29	0.0

[a] These $RuCH_2^+$ results are based on calculations at the GVB(2/4)-RCI level. All quartet states were calculated by using the optimum geometry for $^4A_2$ $RuCH_2^+$, while all doublet-state calculations utilized the optimum geometry for $^2A_2$ $RuCH_2^+$. Ru^+ results are taken from the CI described in Table I, footnote *c*. More accurate $^4A_2$–$^2A_2$ energy splittings are reported in Table V.

a double bond leads to a differential loss of exchange energy of $\Delta K = 1\,K_{sd} + 2.5K_{dd}$. The average s–d exchange interaction in Ru^+ is K_{sd} = 7.5 kcal/mol and the average K_{dd} = 15 kcal/mol, leading to a loss of 45.0 kcal/mol upon forming a double bond. Adding this loss to the promotional energy of 28.4 kcal/mol results in a weakening of the double bond by 73.4 kcal/mol! This suggests that such a state would be high above the ground state.

Repeating the analysis for a double bond comprised of a 5sσ orbital and a 4dπ_{xz} orbital on Ru^+, we find that formation of a double bond to triplet CH_2 leads to a differential exchange energy loss of $\Delta K = 2K_{sd} + 1.5\,K_{dd}$ = 37.5 kcal/mol. Adding the promotional energy yields an inherent weakening of the Ru–C double bond of 65.9 kcal/mol. Thus, if this quartet state is formed at all, we would expect a *weak* $Ru^+{=}CH_2$ bond in which the σ bond involves primarily the 5s orbital on Ru^+.

Summarizing, the formation of covalent bonds to s^1d^6 Ru^+ leads to highly excited states for $Ru{=}CH_2^+$. However, all is not lost: there is yet another possibly favorable manner to form a quartet state. We now consider binding singlet CH_2 to d^7Ru^+. The questions which must be answered for this new case include what sort of bonding is possible, what the costs are concerning promotional and exchange energies, and how these quartet states are related (by symmetry) to our previous constructs.

The bond of singlet CH_2 (**11**, with its doubly occupied sp orbital (σ) in the molecular plane and empty pπ_x orbital perpendicular to the molecular plane) and Ru^+ involves a σ-donor bond from CH_2 to Ru^+ and a possible dπ–pπ "back-bond" from Ru^+ to CH_2. The situation here is slightly more complicated than the usual concept of σ-donor/π-acceptor bonding in which the σ lone pair of the ligand is thought to donate into an empty dσ orbital on the metal, while the metal dπ lone pair delocalizes or "back-bonds" into the empty CH_2 pπ orbital. The complication is that d^7 Ru^+ wishes to be high-spin; the cost in energy to force Ru^+ to have an empty dσ orbital is $2K_{dd}$ = 30 kcal/mol. Thus, it is less favorable to force d^7 Ru^+ into its low-spin configuration than to promote d^7 Ru^+ to s^1d^6 Ru^+. However, promoting Ru^+ does not alleviate the problem, since now the singly occupied 5s orbital is in the σ space, inhibiting σ donation. In addition, high-spin s^1d^6 Ru^+ (^6D) (with all d orbitals occupied) is favored over intermediate-spin s^1d^6 Ru^+ (with a dσ hole) by $1K_{sd} + 3K_{dd}$ = 52.5 kcal/mol. Thus, forcing Ru^+ to have an empty σ orbital is unfavorable by at least 30 kcal/mol. (Furthermore, the $RuCH_2^+$ states formed from such Ru^+ configurations with singlet CH_2 lead to doublet states, whereas we seek quartet states.)

The question now is whether singlet CH_2 can form a good bond to a state with an occupied dσ orbital. Perhaps by mixing in the s^1d^6 excited state, Ru^+ can form a singly occupied 5s–4d$_{z^2}$ hybrid σ orbital which is localized away from the Ru–C bonding area, leaving negligible electron density in the molecular sigma system and thus allowing σ donation from CH_2 ($^1A_1$) into the "vacant" σ space of Ru^+, as shown below. If so, we expect the favorable state to have a doubly occupied dπ_{xz} orbital (to allow dπ–pπ back-bonding) and a singly occupied dσ_{z^2} orbital (to allow s–d hybridzation out the back of the complex so as not to interfere with the σ-donor bond). This leads to three plausible (high-spin) Ru^+ configurations (degenerate for the free ion),

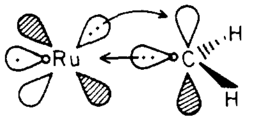

$$(sd\sigma)^1(d\pi)^2(d\bar{\pi})^2(d\delta)^1(d\bar{\delta})^1 \quad (^4A_2)$$

$$(sd\sigma)^1(d\pi)^2(d\bar{\pi})^1(d\delta)^2(d\bar{\delta})^1 \quad (^4B_2)$$

$$(sd\sigma)^1(d\pi)^2(d\bar{\pi})^1(d\delta)^1(d\bar{\delta})^2 \quad (^4B_1)$$

(where the symmetries are for $RuCH_2^+$). These (degenerate) quartet states predicted for Ru^+ (d^7) forming a σ-donor/π-acceptor bond to singlet CH_2 have the same symmetries as for Ru^+ (s^1d^6), forming two covalent bonds to CH_2 $^3(B_1)$! Hence, by calculating the $^4A_2$, $^4B_2$, and $^4B_1$ wave functions for $RuCH_2^+$, we will determine which mode of bonding (donor–acceptor vs. covalent) is preferred.

Of course we can in fact predict a priori which bonding mode is preferred by comparing the promotional and exchange costs for both systems. For covalent bonding we found a total destabilization of 65.9 kcal/mol for forming σ and π bonds utilizing the Ru^+ 5s and 4d$_{xz}$ orbitals. For donor–acceptor bonding, the mixing of some s^1d^6 character into ground-state d^7 Ru^+ will cost no more than the s^1d^6–d^7 promotional energy of 28.4 kcal/mol, and the promotion of CH_2 from triplet to singlet costs 9 kcal/mol,[5] for a total promotional energy of ≤38 kcal/mol. Since no covalent bonds have been formed with Ru^+, we *retain all intraatomic exchange stabilization* on Ru^+. Thus, donor–acceptor bonding is predicted to be more favorable than covalent bonding by 66 − 38 ≥ 28 kcal/mol for the quartet states. This simplistic analysis does not address the probable differences in intrinsic bond stengths of covalent vs. donor–acceptor bonds, as well as the cost of orthogonalizing the singly occupied sdσ orbital away from the donor σ bond. However, with such a large bias toward donor–acceptor bonding due to the retention of exchange terms on Ru^+, we expect that donor–acceptor bonding will be the preferred mode of bonding for the quartet state. The question of where this donor–acceptor state lies relative to the ground state will depend on the two factors neglected in the above analysis: (i) the intrinsic strength of a σ-donor/π-acceptor bond relative to the intrinsic strength of a covalent double bond and (ii) the magnitude of the repulsive interaction in the three-electron σ system.

B. The Quartet State Spectrum for $RuCH_2^+$. From the results in Table IV, we find that the quartet states ($^4A_2$, $^4B_1$, and $^4B_2$) of $RuCH_2^+$ are indeed degenerate, as predicted. In addition, we see that they are not far above the $^2A_2$ ground state of $RuCH_2^+$. The $^4A_2$–$^2A_2$ state splitting as a function of electron correlation is given in Table V, where we see that further inclusion of electron correlation yields a $^4A_2$–$^2A_2$ state splitting of 12.9 kcal/mol. This small state splitting is suggestive of at least two conclusions. First, $RuCH_2^+$ ($^4A_2$) makes use of the least destabilizing mode of bonding available, namely, donor–acceptor bonding, in which little promotional energy and no exchange energy are lost on Ru^+ and only 9 kcal/mol promotional energy is lost by exciting CH_2 from $^3B_1$ to $^1A_1$. Thus we propose that the bonding in $RuCH_2^+$ ($^4A_2$) consists of a σ-donor–π-acceptor bond between CH_2 ($^1A_1$) and Ru^+ (d^7), a description consistent with its molecular properties (vide infra).

The second major conclusion to be drawn from the $^4A_2$ − $^2A_2$ state splitting of 12.9 kcal/mol is that donor/acceptor bond en-

Table V. $^4A_2$–$^2A_2$ Excitation Energies (kcal/mol) for $RuCH_2^+$ [a]

calculational level	no. of config/SEF[b] $^4A_2$	$^2A_2$	$\Delta E(^4A_2-^2A_2)$
HF	1/1	1/1	-20.1
GVB-PP	4/4	8/8	4.9
GVB-RCI	9/34	27/76	15.0
$RCI_\pi{*}D_\sigma + RCI_\sigma{*}D_\pi$	1065/5886	2875/11486	8.9
$(GVB\text{-}RCI{*}S)_{val,Ru}$	442/2570	816/4150	13.0
$(GVB\text{-}RCI{*}S)_{val,full}$	637/4962	1365/8156	14.2
$RCI_\pi{*}D_\sigma + RCI_\sigma{*}D_\pi + (RCI{*}S)_{val,full}$	1579/10042	3895/18102	12.9

[a] Optimum geometries at the GVB(2/4)-RCI level were used for $^2A_2$ and $^4A_2$ $RuCH_2^+$. For excitation energy calculations, the GVB(3/6) level is used for $^2A_2$, while the GVB(2/4) level is used for $^4A_2$, to maintain an "orbitally balanced" description (see section V). [b] No. of config./SEF is the no. of spatial configurations/number of spin eigenfunctions.

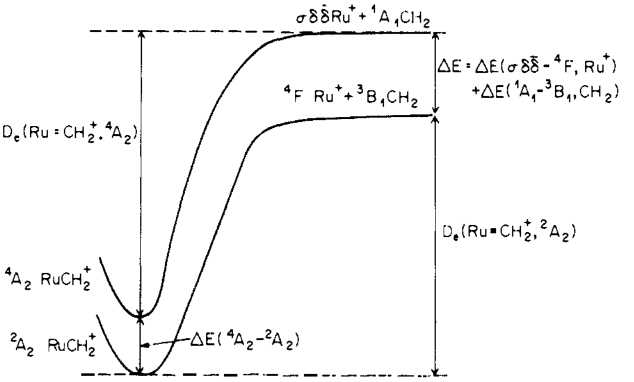

Figure 4. Qualitative potential curves for $^4A_2$ and $^2A_2$ $RuCH_2^+$. Our theoretical values are D_e ($^2A_2$) = 68.0 kcal/mol, D_e ($^4A_2$) = 65.9 kcal/mol, and $\Delta E(^4A_2-^2A_2)$ = 12.9 kcal/mol. Our best estimate for D_e^{exact} ($^2A_2$) = 73.2 kcal/mol.

ergies can be comparable in strength to covalent bond energies. That is, $D_e(Ru{=}CH_2^+, {}^4A_2)$ can be predicted from the cycle illustrated in Figure 4 to be

$$D_e(Ru{=}CH_2^+, {}^4A_2) = D_e(Ru{=}CH_2^+, {}^2A_2) + \Delta E(\sigma\delta\bar{\delta} - {}^4F, Ru^+) + \Delta E({}^1A_1-{}^3B_1, CH_2) - \Delta E({}^4A_2-{}^2A_2)$$

This calculation is explicitly for the *diabatic* bond strength of CH_2 complexes; however, this would be the *adiabatic* bond strength for metal–carbene systems in which the free carbene has a singlet ground state (e.g., CF_2, C(OR)R, etc.) and thus is the relevant quantity to use for comparison with currently observed metal carbenes. The above equation leads to a predicted $D_e(Ru{=}CH_2^+, {}^4A_2)$ of 68.0 + 6.9 + 7.3 − 12.9 = 69.3 kcal/mol,[26] which is of the same magnitude as the covalent $Ru{=}CH_2$ bond strength. Calculated bond energies for $RuCH_2^+$ ($^4A_2$) dissociating to d^7 Ru^+ and CH_2 ($^1A_1$) are discussed in detail in section III.D.

C. Properties of the Low-Lying Excited State, $RuCH_2^+$ ($^4A_2$). It is important to emphasize that it suffices to examine any one of the three degenerate quartet states of $RuCH_2^+$, since they all exhibit the same properties, with the only physical difference between them being the configuration of electrons in nonbonding d orbitals. We choose to examine the $^4A_2$ state simply because it is of the same spatial symmetry as the ground $^2A_2$ state, which allows a more direct comparison of the two spin states.

The optimum geometry for the $RuCH_2^+$ ($^4A_2$) excited state (at the GVB(2/4)-RCI level) is shown in Figure 2b. The Ru–C bond length of 1.93 Å is 0.05 Å longer than the Ru–C bond length in the covalently bonded $^2A_2$ ground state, suggestive of a change in the bonding scheme for the $^4A_2$ state. Supporting evidence that this bond lengthening is due to a change from a covalent (triplet) alkylidene structure to a donor–acceptor (singlet) carbene structure is given by examination of the following experimental example. Roper and co-workers[27] have synthesized and obtained X-ray structures of

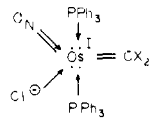

where X = H or F. We would expect the CH_2 case to have an $Os{=}C$ covalent double bond and thus to have nucleophilic, alkylidene character. However, the triplet state of CF_2 is about 46 kcal/mol above the singlet,[28] and hence we would expect electrophilic, carbene character in the latter. The $Os{=}CH_2$ bond length is 1.92 Å,[27a] whereas the $Os{=}CF_2$ bond length is 1.967 Å,[27b] a bond lengthening of 0.047 Å upon going from an alkylidene to a carbene bonding structure. This is in excellent agreement with the bond lengthening of 0.05 Å we find for Ru, lending credence to the assignment of $RuCH_2^+$ ($^4A_2$) as a singlet carbene bound to Ru^+.

Further indication of the singlet nature of the CH_2 ligand in $RuCH_2^+$ ($^4A_2$) is seen in the decrease in HCH bond angle from 121.7° to 113.0°, going from $^2A_2$ to $^4A_2$ $RuCH_2^+$. (The HCH bond angle in CH_2 ($^1A_1$) is 103°, whereas in CH_2 ($^3B_1$) the angle is 133°.[28]) The C–H bond lengths in $RuCH_2^+$ ($^4A_2$) remain the same as in the ground state, R(C–H) = 1.08 Å.

The GVB orbitals for the Ru–C σ and π bonds as well as for the nonbonding singly occupied σ orbital (5s/4dz^2) are shown in Figure 5a. Notice the difference in character of the σ and π bonds of Figure 5a from the covalent σ and π bonds of Figure 1a. The σ bond for $RuCH_2^+$ ($^4A_2$) resembles an "in/out" correlated σ pair of CH_2 ($^1A_1$) (1.27 electrons are localized on CH_2, while the other 0.73 electron is donated to Ru^+), as can be seen by comparing Figure 5a with Figure 5b, which depicts the two σ donor electrons of free CH_2 ($^1A_1$). By comparing Figures 5a and 1a we see also that the π bond for $RuCH_2^+$ ($^4A_2$) has much more character on Ru^+ (1.58 electrons) than does the $RuCH_2^+$ ($^2A_2$) π bond (1.16 electrons). This is consistent with the description of the $RuCH_2^+$ ($^4A_2$) π bond as an "in/out" correlated Ru^+ dπ-orbital backbonding into the empty CH_2 pπ orbital. By comparing the π bond of Figure 5a with the "in/out" correlated two-electron dπ pair in free Ru^+ depicted in Figure 5c, we see that the π bond of $RuCH_2^+$ ($^4A_2$) is indeed a dπ pair on Ru^+ delocalizing onto CH_2. Thus, the σ- and π-bonding orbitals of $RuCH_2^+$ ($^4A_2$) indicate σ-donor/π-acceptor bonding as in **12**. However, recall that high-spin d^7 Ru^+ does not have an empty dσ orbital ready for σ donating by CH_2 ($^1A_1$). The discussion in section III.A proposes that if the singly occupied 4dσ orbital can mix in 5s character to rehybridize away from the Ru–C bond, Ru^+ may simulate an empty dσ orbital by having no electron density in the σ region between Ru and C. The bottom plot of Figure 5a shows this singly occupied Ru^+ orbital, which indeed rehybridizes out the back of the molecule to minimize repulsions with the Ru–C bonds. The Mulliken population of this singly occupied valence orbital show the predicted mixing of the s^1d^6 excited state into the d^7 ground state in order to effect this rehybridization (28% 5s, 72% 4d).

This donor–acceptor bonding mode is further indicated by the Mulliken populations of each bond pair. For the σ bond, there is considerable charge tranfer (0.73 electron) from the CH_2 σ orbital to Ru^+, indicating a strong donor–acceptor interaction. This is complemented in the π system with a "π back-bond" which transfers 0.43 electron back to the CH_2 pπ_x orbital. Because Ru^+ is positively charged, the back-donation from Ru^+ is not as effective as it is expected to be in a saturated, neutral $Ru{=}CH_2$ complex, resulting in a slight overall charge transfer to the metal.

The σ and π bond overlaps in $RuCH_2^+$ ($^4A_2$) provide further verification of our bonding description. In marked contrast to

---

[26] At the highest level of calculation used herein, we find $\Delta E(\sigma\delta\bar{\delta} - {}^4F, Ru^+)$ = 6.9 kcal/mol and $\Delta E({}^1A_1-{}^3B_1, CH_2)$ = 7.3 kcal/mol.

[27] (a) Hill, A. F.; Roper, W. R.; Waters, J. M.; Wright, A. H. *J. Am. Chem. Soc.* **1983**, *105*, 5939. (b) Roper, W. R. "Group VIII Transition Metal Complexes of CH_2, CF_2, and Other Simple Carbenes". Presented at a Seminar at the California Institute of Technology, July 23, 1984.

[28] Bauschlicher, C. W., Jr.; Schaefer, H. F., III; Bagus, P. S. *J. Am. Chem. Soc.* **1977**, *99*, 7106.

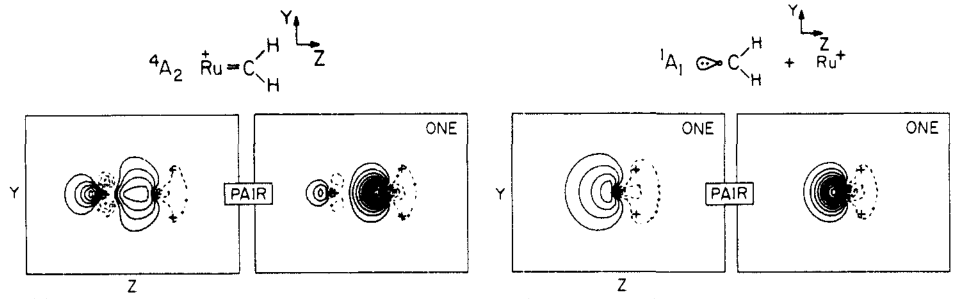

a) (i) CH_2 σ DONOR BOND

b) FREE CH_2 σ LONE PAIR

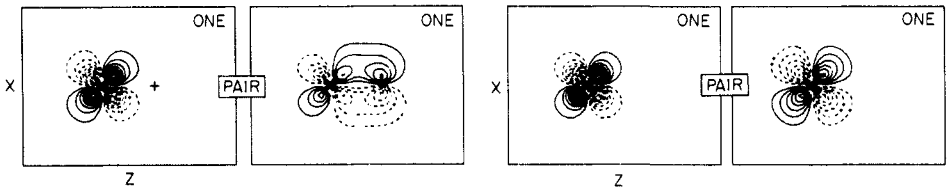

(ii) Ru π BACKBOND

c) FREE Ru^+ dπ LONE PAIR

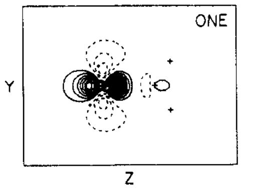

(iii) Ru 4dσ RADICAL ORBITAL

Figure 5. GVB orbitals for (a) the carbene complex $RuCH_2^+$ ($^4A_2$): (i) Ru–C σ bond, (ii) Ru–C π bond, and (iii) Ru sd_{z^2} singly occupied; (b) CH_2 ($^1A_1$) spσ pair; (c) Ru^+ (d^7) $d\pi_{xz}$ pair.

the covalently bonded state of $RuCH_2^+$ ($^2A_2$), which has σ and π bond overlaps of 0.68 and 0.48, respectively, the $RuCH_2^+$ ($^4A_2$) σ and π overlaps are significantly larger, 0.83 for the σ bond and 0.69 for the π bond. This fact by itself is suggestive of bonds more localized over only one center, since an "in/out" correlated σ lone pair on CH_2 ($^1A_1$) has an overlap of 0.85 and a 4d lone pair on Ru^+ has an overlap of 0.93. Thus, the "σ bond" has almost the same overlap as the σ orbital in free CH_2 ($^1A_1$), highly suggestive of a localized σ pair on CH_2 along with a localized π pair on Ru^+ in $RuCH_2^+$ ($^4A_2$).

Even stronger evidence for this donor–acceptor model is provided from the behavior of the overlaps as we stretch the Ru–C bonds, shown in Figure 3. As discussed in section II.B, the overlaps in covalent bonds are expected to decrease monotonically to zero at infinite separation. The overlaps of the Ru–C bond pairs for the $^4A_2$ state exhibit the opposite behavior. Here the overlaps increase as the bond is stretched, with the maximum values reached at the infinite limit [corresponding to the overlaps of the lone pairs in the fragments Ru^+ and CH_2 ($^1A_1$)]. This behavior is completely consistent with our formulation of two lone pairs which delocalize at R_e to form donor–acceptor bonds and relocalize as the bond is broken.

The vibrational frequencies of the $^4A_2$ state are shown in Table II, where we see that the C–H symmetric stretching and scissors bending frequencies are nearly identical with those for the ground state. The only true indicator of a bonding change comes from the much smaller Ru–CH_2 stretching frequency (464 cm^{-1} for the $^4A_2$ state vs. 665 cm^{-1} for the $^2A_2$ ground state). This suggests a looser, if not a weaker, bond (as discussed in the next section), as might be expected intuitively from the nature of a donor–acceptor interaction (not a strong function of distance).

To summarize, all of the properties of the low-lying $^4A_2$ excited state of $RuCH_2^+$ are in sharp contrast to those of the ground-state structure, with the orbitals, geometry, Mulliken populations, dπ–pπ back-bonding interactions, orbital-overlap behavior, and vibrational frequencies completely supporting the description of the bonding in $RuCH_2^+$ ($^4A_2$) as a σ-donor/π-acceptor situation.

D. Bond Energies for $RuCH_2^+$ ($^4A_2$). Donor–acceptor bond strengths for transition-metal systems have presently been limited experimentally to M–CO bond dissociation enthalpies (which range from 37 to 46 kcal/mol[29]). Previous theoretical calculations for transition-metal carbenes have been limited to low-level calculations (HF) using experimental geometries with an MBS (minimum basis set) description of $(CO)_4Cr{=}CH(OH)$ and $(CO)_4Fe{=}CH(OH)$.[30] HF calculations are expected to describe covalent bonds poorly, but may provide acceptable descriptions of donor–acceptor bonds in which the doubly occupied donor orbitals have high overlap. Nakatsuji et al.[30] found bond energies for the above two hydroxycarbenes of 44.4 kcal/mol for the Cr system and 36.8 kcal/mol for the Fe complex at the HF level.

The present bond-energy calculations as a function of electron correlation are given in Table VI. We have chosen here to calculate the (nonadiabatic) bond energy for $RuCH_2^+$ ($^4A_2$) dissociating to the σδδ state of Ru^+ (see Table I) and CH_2 ($^1A_1$). Since Ru^+ and CH_2 adopt these electronic states in the complex, dissociation with geometrical relaxation (i.e., to the equilibrium geometry of singlet CH_2) but no electronic relaxation (e.g., from σδδ to ^4F Ru^+) will yield an intrinsic (promotionless) donor–acceptor bond energy. For comparison with experimental metal–carbene bond energies, this (promotionless) bond energy is the important one, since the metal–carbene bond energy in a saturated metal complex is very likely to involve no electronic relaxation of fragments. For instance, the bond energy in a Fischer carbene complex, e.g., $(CO)_5W{=}C(OMe)Me$, involves the reaction

$$(CO)_5W{=}C(OMe)Me \rightarrow (CO)_5W + :C(OMe)Me.$$

Since both $W(CO)_5$ (low-spin d^6) and C(OMe)Me are expected to be singlets, no electronic relaxation is expected to occur (i.e., $W(CO)_5$ is not likely to relax to a triplet or change its low-spin d^6 orbital occupation). Thus, the bond energy measured for W=C(OMe)Me will involve no promotional energies in the fragments and will therefore be an intrinsic donor–acceptor bond energy. To make a comparison with bond energies for saturated systems, we report electronically nonadiabatic bond energies that (due to the lack of electronic relaxation) correspond to intrinsic

---

(29) Lewis, K. E.; Golden, D. M.; Smith, G. P. *J. Am. Chem. Soc.* **1984**, *106*, 3905.

(30) Nakatsuji, H.; Ushio, J.; Han, S.; Yonezawa, T. *J. Am. Chem. Soc.* **1983**, *105*, 426.

Table VI. Bond Dissociation Energies (kcal/mol) for the Carbene State of $RuCH_2^+$ ($^4A_2$)

calculational level	$D_e(Ru{=}C)$[a]	$RuCH_2^+(^4A_2)$ total energy, hartrees[b]	fragment total energies, hartres	
			Ru^+	$CH_2(^1A_1)$
HF	41.3	−4476.12076 (1/1)	−4437.17331 (1/1)	−38.88164 (1/1)
GVB(2/4)-PP	42.5	−4476.14740 (4/4)	−4437.17741 (2/2)	−38.90231 (2/2)
RCI(2/4)	52.9	−4476.16419 (9/34)	−4437.17763 (3/6)	−38.90231 (2/2)
$RCI_\pi{*}D_\sigma + RCI_\sigma{*}D_\pi$	61.7	−4476.19480 (1065/5886)	−4437.17909 (51/123)	−38.91742 (53/53)
$(RCI(2/4){*}S)_{val,Ru}$	64.0	−4476.20096 (442/2570)	−4437.19659 (57/168)	−38.90231 (2/2)
$(RCI(2/4){*}S)_{val,full}$	70.3[c]	−4476.21696 (637/4962)	−4437.19659 (57/168)	−38.90831 (37/40)
$RCI_\pi{*}D_\sigma + RCI_\sigma{*}D_\pi + (RCI(2/4){*}S)_{val,full}$	65.8	−4476.22638 (1579/10042)	−4437.19808 (101/269)	−38.92342 (79/82)

[a] Bond energy (D_e) dissociating to the $\sigma\bar{\delta}\bar{\delta}$ state of Ru^+ (see Table I) and the $^1A_1$ state of CH_2 [using the optimal GVB(1/2) description for CH_2 (σ/π correlated σ pair)]. [b] The number of spatial configurations/number of spin eigenfunctions are given in parentheses. [c] We believe this value is an overestimate; see discussion in section III.D.

donor–acceptor bond energies.[31,32]

Examination of Table VI reveals that the σ-donor/π-acceptor bond strength (65.8 kcal/mol) in $RuCH_2^+$ ($^4A_2$) is predicted to be nearly as strong as the covalent $D_e(Ru{=}CH_2, {}^2A_2)$ of 68.0 kcal/mol. However, the covalent D_e predicted for a saturated $Ru{=}CH_2$ complex (68.0 + 15 = 83.0 kcal/mol) is larger than the donor–acceptor saturated complex D_e, because the donor–acceptor bond energy as defined does not depend on the degree of saturation (since the metal and CH_2 fragments do not electronically reorganize or change spin couplings).

The progression of bond energies as a function of electron correlation in Table VI indicates a convergence to $D_e(Ru^+{=}CH_2, {}^4A_2) = 65.8$ kcal/mol as our best value for the donor–acceptor intrinsic bond energy of Ru^+ bonding to any carbene (CF_2, CR(OR), CCl_2, etc.). We consider the value of 70.3 kcal/mol for $RCI{*}S_{val,full}$ to be an overestimate of the true bond energy due to an artifact of this particular calculation for donor–acceptor bonding configurations. This level leads to an imbalanced inclusion of electron correlation in which the complex is correlated to a greater degree than the fragments. This is consistent with the large $^1A_1$–$^3B_1$ splitting for CH_2 at this level (16.7 kcal/mol rather than 13.2 kcal/mol as found for other levels), leading to a bond energy which is too high. For covalent bonds, however, this calculational level leads to a fairly balanced description at R_e and $R = \infty$, as borne out in the convergence of covalent bond energies for both $Cr{=}CH_2^+$ ($^4B_1$)[1] and $Ru{=}CH_2^+$ ($^2A_2$).

In summary, we predict donor–acceptor bonds of typical (singlet) carbenes such as $:CF_2$, $:CCl_2$, :CR(OR), etc., to Ru to have bond strengths of ~65 kcal/mol, while covalent Ru=C alkylidene bond strengths in saturated complexes are expected to be ~85 kcal/mol. In addition, since $Ru{=}CF_2$ and other ruthenium-carbene complexes have been synthesized by Roper and co-workers,[33] while terminal Ru–CR_2 alkylidene systems are as yet unknown (although postulated by Knox,[34] Werner,[22] and Shapley[35]), this suggests a lower bound on an Ru–C single (covalent) bond energy of ≥43 kcal/mol. We conclude this simply by observing that many μ-CR_2–Ru complexes exist, with two Ru–C σ bonds in preference to terminal $Ru{=}CR_2$ complexes.[34-36] Thus, two Ru–C σ bonds are more stable than one 86 kcal/mol Ru=C terminal double bond, which implies $D(Ru\text{–}C) \geq 43$ kcal/mol.

IV. Summary

Ab initio electronic structure calculations on $RuCH_2^+$ reveal the following conclusions:

i) $RuCH_2^+$ has a $^2A_2$ ground state with two covalent Ru–C bonds, resulting in a bond energy of 68.0 kcal/mol for the unsaturated metal–CH_2 complex.

ii) From the present calculations and others on more saturated complexes, a means of estimating covalent-bond energies for fully saturated metal complexes from bond energies known for unsaturated complexes is put forth, with the result

$$D_{saturated} = D_{intrinsic} - \tfrac{1}{2}K_{dd} = D_{unsaturated} + \Delta K_{lost} - \tfrac{1}{2}K_{dd}$$

In particular, this yields an estimate for an $Ru{=}CH_2$ bond energy in a coordinatively saturated complex of 83.0 kcal/mol, which agrees well with a model saturated $Ru{=}CH_2$ complex (with a calculated bond energy of 85.5 kcal/mol).

iii) A low-lying (12.9 kcal/mol up) triply degenerate excited state exists ($^4A_2$, $^4B_1$, $^4B_2$) with an Ru–C double bond of completely different structure from the ground state; namely, the excited state exhibits metal–carbene σ-donor/π-acceptor bonding. This donor/acceptor bond is worth 65.8 kcal/mol for both unsaturated and saturated complexes.

iv) A lower bound of 43 kcal/mol is obtained for the covalent Ru–C single bond strength in a saturated complex.

V. Calculational Details

A. Basis Sets. All atoms were described with all-electron valence double-ζ (VDZ) basis sets. In addition, one set of d-polarization functions ($\zeta_d = 0.69$) was added to the C basis set.[1] A Four's level VDZ basis set was used for Ru with the (16s13p7d/6s5p3d) contraction, shown in Table VII.[37] The Ru and Ru^+ state splittings obtained with this basis set contraction at the HF level are given in Table VIII. The standard Huzinaga–Dunning VDZ bases were used for C (9s5p/3s2p) and H (4s/2s).[38]

B. Geometry Optimizations. All geometrical parameters of the $^4A_2$ and $^2A_2$ states of $RuCH_2^+$ were optimized at the GVB-RCI(2/4) level (generalized valence bond–restricted configuration interaction). The GVB-RCI(2/4) description allows a full CI within each pair of natural orbitals (NO's, two natural orbitals

---

[31] No exchange energy is lost upon bonding in these complexes. Thus the intrinsic bond energy for a donor–acceptor bond is "promotionless" instead of "exchangeless".

[32] To calculate an adiabatic bond energy for $RuCH_2^+$ ($^4A_2$) merely involves $D_e(^2A_2) - \Delta E(^4A_2\text{–}^2A_2)$ (see Figure 4).

[33] (a) Clark, G. R.; Hoskins, S. V.; Jones, T. C.; Roper, W. R. *J. Chem. Soc., Chem. Commun.* **1983**, *719*. (b) Clark, G. R.; Hoskins, S. V.; Roper, W. R. *J. Organomet. Chem.* **1982**, *234*, C9. (c) Hoskins, S. V.; Pauptit, R. A.; Roper, W. R.; Waters, J. M. *Ibid.* **1984**, *269*, C55. (d) Roper, W. R.; Wright, A. H. *Ibid.* **1982**, *233*, C59.

[34] Dyke, A. F.; Knox, S. A. R.; Mead, K. A.; Woodward, P. *J. Chem. Soc., Chem. Commun.* **1981**, *861*; and paper immediately following.

[35] Holmgren, J. S.; Shapley, J. R. *Organometallics* **1985**, *4*, 793.

[36] Lin, Y. C.; Wreford, S. S. *J. Am. Chem. Soc.* **1983**, *105*, 1679.

[37] Rappé, A. K.; Goddard, W. A., III, to be published. This basis set was optimized for the d^n configuration of the metal as laid out in Rappé, A. K.; Smedley, T. A.; Goddard, W. A., III *J. Phys. Chem.* **1981**, *85*, 2607. The 4d VDZ basis optimized in this manner is an adequate description of the valence space.

[38] (a) Huzinaga, S. *J. Chem. Phys.* **1965**, *42*, 1293; (b) Dunning, T. H., Jr. *Ibid.* **1970**, *53*, 2823.

Table VII. The Ru Basis Set (ref. 37): Cartesian Gaussian Functions with Exponents (α_i) and Contraction Coefficients (C_i)

function type	α_i	C_i
s	24880.0	0.0200127
s	3752.0	0.1389632
s	848.1	0.4836489
s	231.5	0.4952994
s	331.7	−0.1331553
s	60.94	0.4216589
s	24.01	0.6727022
s	35.38	−0.3054903
s	9.385	0.4059748
s	3.929	0.7725757
s	5.203	−0.4048137
s	1.285	0.6905008
s	0.4972	0.5490496
s	0.7682	−0.5317929
s	0.09777	1.1559939
s	0.03488	1.0000000
p	1212.0	0.0286098
p	284.7	0.1876312
p	88.76	0.5223895
p	30.9	0.4279650
p	20.06	0.0639444
p	11.68	0.5004604
p	4.489	0.5127291
p	9.097	−0.0409377
p	1.534	0.6317161
p	0.5207	0.4622364
p	0.8698	−0.2023235
p	0.1292	1.0568153
p	0.04051	1.0000000
d	136.9	0.0446661
d	39.33	0.2414630
d	13.58	0.5272307
d	4.817	0.4114895
d	3.873	0.1958215
d	1.281	0.8701024
d	0.3139	1.0000000

Table VIII. Hartree–Fock State Splittings for Ru and Ru$^+$ [a]

state	total energy, hartrees	excitation energies (eV)		
		this work	NHF[b]	expt[c]
Ru(^{3}F)	−4437.30190	2.61	1.69	1.09
Ru(^{5}D)	−4437.35033	1.30	1.42	0.87
Ru(^{5}F)	−4437.39794	0.00	0.00	0.00
Ru$^+$(^{6}D)	−4437.13866	7.06	7.10	8.46
Ru$^+$(^{4}F)	−4437.18354	5.83	5.92	7.37

[a] Results are for the Ru basis set contraction shown in Table VII. [b] Numerical Hartree–Fock results from ref 39. [c] Experimental data from ref 25, averaged over angular momentum states.

per M–C bond) describing the Ru–C σ and π bonds, resulting in nine spatial configurations. For $^2A_2$ $\mathrm{RuCH_2}^+$ these nine configurations have 17 associated spin eigenfunctions (SEF's), while for the $^4A_2$ state the nine configurations have 34 associated SEF's. The physical interpretation of the RCI wave function involves inclusion of interpair correlation and high-spin coupling on the metal atom.

C. Bond Energies. 1. $\mathrm{RuCH_2}^+$ ($^2A_2$): Covalent Bonds. Bond energies for $\mathrm{RuCH_2}^+$ were calculated at the Hartree–Fock (HF), generalized valence bond with perfect-pairing restriction [GVB](2/4)-PP, GVB-RCI(2/4), $\mathrm{RCI}_\pi*\mathrm{D}_\sigma + \mathrm{RCI}_\sigma*\mathrm{D}_\pi$, RCI(2/4)$*\mathrm{S}_{\mathrm{val,Ru}}$, RCI(2/4)$*\mathrm{S}_{\mathrm{val,full}}$, and $[(\mathrm{RCI}_\pi*\mathrm{D}_\sigma + \mathrm{RCI}_\sigma*\mathrm{D}_\pi)$ + RCI(2/4)$*\mathrm{S}_{\mathrm{val,full}}]$ levels. The bond energies given in Table III are for the adiabatic dissociation pathway

$$\mathrm{Ru{=}CH_2}^+\ (^2A_2) \rightarrow \mathrm{Ru}^+\ (^4F) + \mathrm{CH_2}\ (^3B_1)$$

Calculations at large R(Ru–C) distances (e.g., 5.00 Å) indicate that the $\sigma^1\pi^1\delta^1$ configuration of Ru$^+$ at R_e smoothly converts into ^{4}F Ru$^+$ at large R, giving rise to a truly adiabatic potential energy pathway. We now define the higher order CI's listed above:

1) $\mathrm{RCI}_\pi*\mathrm{D}_\sigma + \mathrm{RCI}_\sigma*\mathrm{D}_\pi$: From the nine RCI configurations for $\mathrm{RuCH_2}^+$ ($^2A_2$), we allow all single and double excitations to all virtuals from one Ru–C bond pair at a time, while maintaining the RCI description in the other bond pair. In particular, while the Ru–C π bond is described at the RCI level, we simultaneously allow all single and double excitations from the Ru–C σ bond pair and then vice versa, hence the name $\mathrm{RCI}_\pi*\mathrm{D}_\sigma + \mathrm{RCI}_\sigma*\mathrm{D}_\pi$. This CI dissociates properly to HF fragments. (Note that all single and double excitations from both bond pairs simultaneously do not dissociate to a cleanly described limit.)

2) RCI(2/4)$*\mathrm{S}_{\mathrm{val,Ru}}$: From the nine RCI configurations we allow all single excitations from the valence Ru orbitals and the Ru–C bonds to all virtuals. This CI is also dissociation-consistent, dissociating to HF$*\mathrm{S}_{\mathrm{valence}}$ for Ru$^+$ and HF for CH$_2$.

3) RCI(2/4)$*\mathrm{S}_{\mathrm{val,full}}$: From the nine RCI configurations we allow all single excitations from all valence orbitals (including CH pairs) to all virtuals. We allow this CI to dissociate to HF$*\mathrm{S}_{\mathrm{val}}$ fragments, although this is overcorrelating the dissociated limit and thus will give too small a bond energy. Test calculations indicate this leads to at most a 0.2 kcal/mol underestimate of the bond energy.

4) $[(\mathrm{RCI}_\pi*\mathrm{D}_\sigma + \mathrm{RCI}_\sigma*\mathrm{D}_\pi)$ + (RCI(2/4)$*\mathrm{S}_{\mathrm{val,full}}$)]: This CI is merely the superposition of the previous two CI's listed above, dissociating to HF$*\mathrm{S}_{\mathrm{val}}$ fragments, with the same slight overcorrelation problem resulting in ~0.2 kcal/mol too low a bond energy.

2. $\mathrm{RuCH_2}^+$ ($^4A_2$): Donor/Acceptor Bonds. The bond energies for the $^4A_2$ state were calculated at the same levels as the ground state; thus the CI's are identical at R_e for both states. However, this state dissociates to CH$_2$ ($^1A_1$) and $\sigma\delta\bar{\delta}$ Ru$^+$ (since the electronic configuration of Ru$^+$ at R_e does not change upon stretching this type of bond). We allow the CH$_2$ σ pair to use a π-correlating orbital as a second natural orbital, since this is the optimum GVB(1/2) description of singlet CH$_2$. Note that at R_e, π back-bonding from Ru$^+$ forces the dominant correlating orbital to be σ^* for the CH$_2$ σ pair. Thus the dominant correlation changes from R_e to $R = \infty$, and we allow the optimal correlation for both limits. We now discuss the CI's in terms of their dissociation limits, since these limits are different from the covalent case.

1) $\mathrm{RCI}_\pi*\mathrm{D}_\sigma + \mathrm{RCI}_\sigma*\mathrm{D}_\pi$: This CI dissociates to a GVB(1/2)-correlated Ru$^+$ dπ pair and a GVB(1/2)-correlated CH$_2$ σ pair, from each of which all single and double excitations to all virtuals are allowed. This overcorrelates the infinite limit (since simultaneous double excitations on both fragments result in overall quadruples), leading to a lower bound on the bond energy. However, test calculations at $R = \infty$ show these quadruple excitations do not contribute to the bond energy. Thus the bond energy is effectively dissociation-consistent.

2) RCI(2/4)$*\mathrm{S}_{\mathrm{val,Ru}}$: This wave function dissociates properly to RCI(1/2)$*\mathrm{S}_{\mathrm{val}}$ on Ru$^+$ and RCI(1/2) on CH$_2$ ($^1A_1$).

3) RCI(2/4)$*\mathrm{S}_{\mathrm{val,full}}$: This wave function dissociates to RCI(1/2)$*\mathrm{S}_{\mathrm{val}}$ Ru$^+$ and RCI(1/2)$*\mathrm{S}_{\mathrm{val}}$ CH$_2$, which provides a lower bound on the bond energy, but in practice, test calculations suggest this overcorrelation is negligible (<0.02 kcal/mol).

4) $[(\mathrm{RCI}_\pi*\mathrm{D}_\sigma + \mathrm{RCI}_\sigma*\mathrm{D}_\pi)$ + (RCI(2/4)$*\mathrm{S}_{\mathrm{val,full}}$)]: The superposition of the two CI's above dissociates to [(RCI(1/2)$*\mathrm{D}_\pi$) + (RCI(1/2)$*\mathrm{S}_{\mathrm{val}}$)] Ru$^+$ and [(RCI(1/2)$*\mathrm{D}_\sigma$) + (RCI(1/2)$*\mathrm{S}_{\mathrm{val}}$)] CH$_2$. Again this wave function involves higher order excitations at $R = \infty$ that are not included at R_e, resulting in a net overcorrelation of 0.3 kcal/mol from test calculations.

5) "Test Calculations": We superimpose the two fragment wave functions without allowing any electronic interaction between them, to simulate the infinitely far apart fragments. Then we perform the same CI's for this superimposed fragment wave function as were calculated at R_e. This provides a check on potential overcorrelation problems. The largest difference between the "test" bond energies and the bond energies calculated from the (sometimes overcorrelated) fragments was 0.3 kcal/mol.

D. State Splitings. The $^4A_2$ state at the GVB(2/4)-PP level has a valence space consisting of two C–H doubly occupied orbitals

---

(39) Martin, R. L.; Hay, P. J. *J. Chem. Phys.* **1981**, *75*, 4539.

(treated as HF MO's), two Ru–C bond pairs each with a second NO for a total of four Ru–C bonding orbitals, one doubly occupied nonbonding $d\pi_{yz}$ orbital, and three singly occupied $d\sigma$, $d\delta$, $d\bar{\delta}$ orbitals, for a total of 10 orbitals in the valence space. At the GVB(2/4)-PP level for $RuCH_2^+$ ($^2A_2$), there is the same orbital space for CH_2 and for the Ru–C bonds, but there are two doubly occupied nonbonding d orbitals ($d\pi_{yz}$ and $d\delta_{x^2-y^2}$) plus one singly occupied $d\delta_{xy}$ orbital, for a total of nine valence orbitals. To treat the states of $RuCH_2^+$ with the same degree of flexibility, we must have the same number of valence orbitals in the SCF calculations. Therefore, for $RuCH_2^+$ ($^2A_2$) we correlate the $d\delta_{x^2-y^2}$ with a second natural orbital (leading to a GVB(3/6)-PP description) in order to compare with the GVB(2/4)-PP description of $RuCH_2^+$ ($^4A_2$).

Acknowledgment. This work was supported by the Shell Development Company, Houston, TX, and the National Science Foundation (Grant No. DMR82-15650).

Registry No. $Ru{=}CH_2^+$, 101031-94-1.

Thermal Decomposition of Silane

Mark S. Gordon,*[†] David R. Gano,[‡] J. Stephen Binkley,[⊥] and Michael J. Frisch[‖]

Contribution from the Department of Chemistry, North Dakota State University, Fargo, North Dakota 58105, Department of Chemistry, Minot State College, Minot, North Dakota, Sandia National Laboratory, Livermore, California 94550, and Analytical Sciences Division, Kodak Research Laboratories, Rochester, New York 14650.

Received September 13, 1985

Abstract: The essential features of the potential energy surface for the thermal decomposition of silane have been calculated with extended basis sets, augmented by correlation corrections. It is predicted that the transition state for the molecular elimination lies 56.9 kcal/mol above silane. For the reverse reaction, the transition state is less than 2 kcal/mol above the separated fragments, silylene and molecular hydrogen, but 4.8 kcal/mol above a long-range potential well. In the latter, the silylene–H_2 separation is 1.78 Å, and the bond in H_2 has stretched by more than 0.05 Å. This indicates a significant electronic interaction between the fragments even at the large fragment separation. The depth of the well is less than 1 kcal/mol at the SCF level of theory, but it increases substantially when correlation is introduced into the wave function. Since the calculated SiH bond energy is 22 kcal/mol larger than the activation energy for the molecular elimination, the homolytic cleavage of silane to form silyl radical is not expected to be an important process in the low-energy pyrolysis of silane.

I. Introduction

The mechanism of the thermal decomposition of silane is of considerable current interest. Silane decomposition is the initial chemical step in the chemical vapor deposition (CVD) of silicon on surfaces. At low temperatures, the primary decomposition process in silane pyrolysis is the elimination of molecular hydrogen to form silylene.[1]

$$SiH_4 \rightarrow SiH_2 + H_2 \qquad (1)$$

The latter species is the simplest example of divalent silicon, a class of compounds with great mechanistic importance in organosilicon chemistry. In the current context, for example, silylene may insert into an Si–H bond of the parent to form disilane, thereby allowing the study of the thermal decomposition mechanisms of this molecule as well.[2]

John and Purnell[3] (JP) have estimated the heat of formation of silylene to be 57.9 kcal/mol, while O'Neal and Ring[4] (OR), based on their silane and disilane pyrolysis experiments, find just over 58 kcal/mol for this quantity. Combined with the heat of formation of 8.2 kcal/mol for silane,[5] this suggests that the endothermicity of (1) is about 50 kcal/mol. JP and OR estimate the activation energy E_a for the insertion of silylene into H_2 [the reverse of (1)] to be 5 and 8 kcal/mol, respectively. This suggests a decomposition barrier of 55–58 kcal/mol for silane. Jasinski and Estes,[6a] using the technique of laser powered homogeneous pyrolysis, have directly determined the latter E_a to be 52 ± 7 kcal/mol and have very recently determined the activation energy for the insertion of silylene into D_2 to be 1 kcal/mol.[6b]

There have been several theoretical studies of reaction 1. Viswanathan, Thompson, and Raff[7] (VTR) have used a semiempirical potential energy surface to predict the kinetics of the unimolecular decomposition of silane and concluded that the channel corresponding to homolytic cleavage of one SiH bond only becomes important at internal silane energies in excess of 5.0 eV. Gordon,[8] using second-order Møller–Plesset perturbation (MP2) theory and the 6-31G* basis set,[9] found an insertion barrier of 8.6 kcal/mol. With third-order perturbation theory (MP3) and polarization functions on the hydrogens (6-31G** basis set[9]), the barrier is reduced to 5.5 kcal/mol.[10] Correcting for zero-point vibrational contributions raises these values by about 2 kcal/mol, resulting in activation energies of 10.6 and 7.5 kcal/mol, respectively. The latter value is within the range of the experimental estimates.

Using a double-ζ plus polarization basis set, Grev and Schaefer[11] (GS) have studied reaction 1 with a two-configuration multiconfigurational self-consistent-field (MCSCF) wave function, augmented by second-order configuration interaction (SOCI). This 7000 configuration wave function predicts a 6.8 kcal/mol

---

[†] North Dakota State University.
[‡] Minot State College.
[⊥] Sandia National Laboratory.
[‖] Kodak Research Laboratories.

(1) (a) Purnell, J. H.; Walsh, R. *Proc. R. Soc. London* **1966**, *A293* 543. (b) Neudorfl, P.; Jodhan, A.; Strausz, O. P. *J. Phys. Chem.* **1980**, *84*, 338. (c) Newman, C. G.; O'Neal, H. E.; Ring, M. A.; *Leska*, E. F.; Shipley, N. *Int. J. Chem. Kinet.* **1979**, *11*, 1167.

(2) Olbrich, G.; Potzinger, P.; Reimann, B.; Walsh, R. *Organometallics* **1984**, *3*, 1267.

(3) John, P.; Purnell, J. H. *J. Chem. Soc., Faraday Trans. 1*, **1973**, *69*, 1455.

(4) O'Neal, H. E.; Ring, M. A. *Chem. Phys. Lett.* **1984**, *107*, 442.

(5) Chase, M. W.; Curnutt, J. L.; Downey, J. R.; McDonald, R. A.; Syverud, A. N.; Valenzuela, E. A. *J. Phys. Chem. Ref. Data* **1982**, *11*, 695.

(6) (a) Jasinski, J. M.; Estes, R. D. IBM Research Report No. 49067, 1985. (b) Jasinski, J. M. *J. Phys. Chem.*, submitted.

(7) Viswanathan, R.; Thompson, D. L.; Raff, L. M. *J. Chem. Phys.* **1984**, *80*, 4230.

(8) Gordon, M. S. *J. Chem. Soc., Chem. Commun.* **1981**, 890.

(9) Hariharan, P. C.; Pople, J. A. *Theor. Chim. Acta* **1973**, *28*, 213. Gordon, M. S. *Chem. Phys. Lett.* **1980**, *76*, 163.

(10) Gordon, M. S.; Gano, D. R. *J. Am. Chem. Soc.* **1984**, *106*, 5421.

(11) Grev, R. S.; Schaefer, H. F., III *J. Chem. Soc., Chem. Commun.* **1983**, *14*, 785.

0002-7863/86/1508-2191$01.50/0